

University of Nebraska - Lincoln

DigitalCommons@University of Nebraska - Lincoln

Theses, Dissertations, and Student Research from
Electrical & Computer Engineering

Electrical & Computer Engineering, Department of

Spring 4-21-2017

5G-UCDA Multi Antenna-To-Logical Cell Circular FIFO Mapping Strategy For High-Speed Train Wireless Communications

Subharthi Banerjee

University of Nebraska-Lincoln, sbanerjee5@unl.edu

Follow this and additional works at: <http://digitalcommons.unl.edu/elecengtheses>



Part of the [Power and Energy Commons](#), [Signal Processing Commons](#), and the [Systems and Communications Commons](#)

Banerjee, Subharthi, "5G-UCDA Multi Antenna-To-Logical Cell Circular FIFO Mapping Strategy For High-Speed Train Wireless Communications" (2017). *Theses, Dissertations, and Student Research from Electrical & Computer Engineering*. 76.
<http://digitalcommons.unl.edu/elecengtheses/76>

This Article is brought to you for free and open access by the Electrical & Computer Engineering, Department of at DigitalCommons@University of Nebraska - Lincoln. It has been accepted for inclusion in Theses, Dissertations, and Student Research from Electrical & Computer Engineering by an authorized administrator of DigitalCommons@University of Nebraska - Lincoln.

5G-UCDA MULTI
ANTENNA-TO-LOGICAL CELL CIRCULAR FIFO
MAPPING STRATEGY FOR HIGH-SPEED TRAIN WIRELESS
COMMUNICATIONS

By

Subharthi Banerjee

A THESIS

Presented to the Faculty of

The Graduate College at the University of Nebraska

In Partial Fulfillment of Requirements

For the Degree of Master of Science

Major: Telecommunications Engineering

Under the Supervision of Professor Hamid R. Sharif-Kashani

Lincoln, Nebraska

May 2017

5G-UCDA MULTI ANTENNA-TO-LOGICAL CELL CIRCULAR FIFO MAPPING
STRATEGY FOR HIGH-SPEED TRAIN WIRELESS COMMUNICATIONS

Subharthi Banerjee, M.S.

University of Nebraska, 2017

Advisor: Hamid R. Sharif-Kashani

2020 is the target year for the roll out of fifth generation wireless communication methodologies. The commercial vendors have characterized 5G as a collection of disruptive set of technologies to provide high throughput, low latency communication supporting a variety of services, i.e., machine to machine communication to next generation base stations and vehicle-to-vehicle communication to radio-over-fiber and high mobility channels. High-speed train wireless communication channels as a subset of high mobility channels have their clear advantages and disadvantages considering other vehicular channels. The speed of high-speed trains is going to reach 500km/hr and with Hyperloop it may reach 1000km/hr. LTE for railways (have) has been specified to support train to ground communication channels only up to 350km/hr and is still not future proof considering the bandwidth intensive passenger services. The next generation passenger services include conference calls, Ultra-HD video streaming, 360° video streaming and downloads, resource intensive multimedia services for passengers comprising of gaming, personalized advertising, virtual and augmented reality, etc. Therefore, high-speed trains being next generation transportation system, the services provided to passengers on-board may suffer compared to the ground. The difference in provided services may sound significant compared to in-flight infotainment services based on satellite communication and on-board Wi-Fi.

In our approach, we have investigated the 5G physical deployment scenario without disrupting or interfering with prioritized train control communication channels. The novelty of separating train control and passenger services can be observed with mapping of different planes in 5G/LTE evolution specification. The separation provides an opportunity to not to compromise passenger services, maintaining quality of service in resource sensitive bandwidth. In our study, we found out that with more number of physical small cell deployment, capacity and area spectral efficiency are biased in front of base stations. In most of the conventional architectures the reliability and bandwidth efficiency of the architecture degrade beyond $-2 \times \text{standard deviation}$ according to Gaussian distribution, which is directly related to propagation distance. In our proposed architecture, we showed that with a deployment scheme of on-roof multi train antennas, physical size of small cells can be reduced further and adaptably extended based on antenna distances. The on-roof antennas connected through fiber can access small cells in First In First Out manner without any additional signaling overhead or forwarding. The scope of this adaptability reduces outage probability comparable to macro cells and achieves flexible power consumption with high area spectral efficiency. The proposed architecture can attain a 10-15-fold improvement in spectral efficiency and 95% improvement in reliability than conventional architectures.

Copyright 2017, Subharthi Banerjee

Dedicated to my family, friends, members of TEL and High-speed Train fans all over the world.

Acknowledgments

I would, first and foremost, like to thank my advisor Dr. Sharif for his invaluable guidance, support and inspiration during the course of my research work. I am also thankful to my colleague Sushanta for his help and support during the time I was working on this research. I would specially like to mention Dr Hempel for his continuous inputs and constant guidance towards future directions to make the project into a success. Finally, I am very thankful to Dr Xiaoyue Cheng for her comments and review regarding statistical algorithm building.

I would like to sincerely thank the Federal Railroad Administration (FRA) for their generous funding of the project that has led to this research.

Although no amount of gratitude can ever be enough for them but still I would like to thank my parents for their unwavering support and belief in my dreams. I would not be here today writing these words without their constant inspiration and encouragement. I would also take a moment to say a big cheer to all of my friends without whom the journey would not have been so easy and inspiring.

Table of Contents

List of Figures	xi
List of Tables	xiv
List of Acronyms	xv
Chapter 1. INTRODUCTION TO HIGH-SPEED TRAIN COMMUNICATION	
CHANNELS	
.....	1
1.1.Importance of High-speed Train.....	1
1.2.High-speed Train Communication channel scenario	3
1.2.1. Time Varying Channels.....	5
1.2.2. Large and Small Scale Fading.....	6
1.2.3. Nonstationarity of the HST Communication Channel.....	7
1.3.Challenges in HST communication	8
1.3.1. Doppler Shift & Doppler Spread.....	9
1.3.2. Inter Carrier Interference	11
1.3.3. Fast Handover	11
1.3.4. Delay Spread.....	12
1.3.5. Linear Coverage.....	13
1.3.6. Sparse Multipath.....	14
1.3.7. Train Car Related Issues	14
1.4.Envisioning Next Generation Wireless Communication for High-speed Ground Mobility.....	15
Chapter 2. COMMUNICATION METHODOLOGIES IN HST	16
2.1.GSM-R to LTE-R	16

2.1.1. GSM-R.....	16
2.1.2. GSM-R Services.....	16
2.1.3. LTE-R.....	17
2.1.4. LTE-R Services.....	19
2.2. Architecture Consideration.....	21
2.2.1. Radio Over Fiber.....	22
2.2.1.1. Access Network.....	23
2.2.1.2. Moving Extended Cell.....	24
2.2.1.3. Moving Frequency Cell Conc.....	24
2.2.1.4. Optical Switching	25
2.2.1.5. Distributed Antenna and Remote Antenna Units.....	25
2.2.2. Small Cells	27
2.2.3. Coordinated Multipoint (CoMP)	29
2.2.4. User and Control Plane Decoupled Architecture.....	30
2.2.5. On-Roof Antennas and RADIATE.....	31
Chapter 3. 5G PHYSICAL LAYER CONDITIONS	33
3.1 Architecture Consideration.....	34
3.1.1 5G in High-speed Train.....	36
3.1.1.1 Channel Variations and Estimations.....	37
3.1.1.2 Signal Processing.....	37
3.1.1.3 Large Scale Fading in mmWave	37
3.2 Key Technologies in 5G.....	42
3.2.1 Densification.....	42
3.2.2 Massive MIMO.....	43

3.2.3	Stationarity and Nonstationarity.....	44
3.2.4	Beamforming.....	45
3.2.5	Waveforms.....	46
Chapter 4. WAVEFORMS IN 5G		47
4.1	Waveform Candidates.....	48
4.1.1	FBMC.....	49
4.1.1.1	Advantages.....	50
4.1.1.2	Disadvantages.....	51
4.1.2	UFMC.....	51
4.1.2.1	Advantages.....	53
4.1.2.2	Disadvantages.....	53
4.1.3	GFDM	54
4.1.3.1	Advantage	55
4.1.3.2	Disadvantage	56
4.2	Selecting Waveform Candidates for HST Environment.....	56
4.3	A Comparative Result with FBMC.....	57
4.4	NYU Simulator.....	58
Chapter 5. USER AND CONTROL PLANE DECOUPLED ARCHITECTURE (UCDA).....		60
5.1	The UCD Architecture.....	60
5.1.1	Phantom Cells.....	62
5.1.2	LTE Frames.....	62
5.1.2.1	Frames and Channel Mapping.....	63
5.1.2.2	Framing in PHY Layer.....	65

5.1.3 UCDA and HST.....	65
5.2 Analysis of the Architecture.....	66
5.2.1 Reliability of the Architecture.....	67
5.2.1.1 Outage Probability.....	67
5.2.1.2 Unreliability Factor.....	68
Chapter 6. MULTI-ANTENNA CIRCULAR FIBER-FED FIFO FOR LOGICAL CELL MAPPING (MAC-3FLCM)	70
6.1 Background.....	71
6.2 Problem Statement.....	72
6.3 The Proposed Architecture.....	74
6.3.1 Logical Cells.....	75
6.3.2 Proposed Handover Scheme.....	78
6.3.3 Power Control	82
6.4 Analysis of the Proposed Scheme.....	82
6.5 Simulation Results.....	86
6.6 Discussions.....	89
6.7 Future Work.....	91
6.8 Conclusions.....	91
REFERENCES	92

List of Figures

Figure 1.1: Different HST environment scenarios: (a) Viaduct, (b) Cutting, (c) Tunnel	4
Figure 1.2: Train movement and simple ray tracing	5
Figure 1.3: Shadow fading in different HST environment scenarios	7
Figure 1.4: Doppler shift for $f_c = 28$ GHz and $v = 300$ and 1000 km/hr	10
Figure 1.5: Hard handover scenario.....	12
Figure 2.1: LTE-R Frequency allocation in different continents	18
Figure 2.2: LTE-R architecture with backwards GSM-R compatibility	20
Figure 2.3: RoF ring distributed and WDM optical switched network.....	23
Figure 2.4: Moving Extended Cell Concept	24
Figure 2.5: Moving Frequency Cell Concept	24
Figure 2.6: Small cell based network	28
Figure 2.7: CoMP architecture	29
Figure 2.8: Conventional UCDA	30
Figure 2.9: RADIATE architecture	31
Figure 3.1: IMT-A (2020) goals	33
Figure 3.2: 5G device centric architecture	34
Figure 3.3: Free Space Path Loss (mmWave).....	38
Figure 3.4: Street Canyon UMa pathloss model for $f_c = 28$ and 73 GHz.....	40

Figure 3.5: Rainloss for mmWave frequencies	39
Figure 4.1: FBMC transmitter blocks	49
Figure 4.2: Waveform PSD comparison between FBMC and OFDM	50
Figure 4.3: UFMC transceiver design.....	52
Figure 4.4: UFMC waveform with 10 subbands.....	53
Figure 4.5: GFDM transmitter.....	54
Figure 4.6: GFDM receiver (a) and waveform (b)	55
Figure 4.7: Emulation setup for High-speed mobility	57
Figure 4.8: NYU Wireless Simulation Results	57
Figure 5.1: Conventional LTE frame structure.....	64
Figure 5.2: LTE proposed frame structure	64
Figure 5.3: Complete Architecture of UCDA.....	66
Figure 5.4: Frame mapping and relations.....	68
Figure 6.1: Handover scenario in UCDA for overlapping region	73
Figure 6.2: Propagation distance variance in UCDA.....	75
Figure 6.3: MAC-3FLCM logical cell.....	76
Figure 6.4: CoMP handover for proposed MAC-3FLCM.....	80
Figure 6.5: Comparison of capacity in the proposed architectures	86
Figure 6.6: Comparison of outage probability in the architectures.....	87

Figure 6.7: Comparison of outage probability in different architectures based on cell
radius..... 88

List of Tables

Table 1.1: Scene Partition for HST Environments.....	4
Table 1.2: Phase Change tracking for HST environment.....	6
Table 2.1: Comparison among radio access methods.....	19
Table 3.1: Comparison of ICI mitigation techniques	36
Table 5.1: Comparison between SDN and UCDA.....	62
Table 6.1: MAC-3FLCM logical cell mapping	78
Table 6.2: Simulation parameters	86

List of Acronyms

3GPP	Third Generation Partnership Project
5G	Fifth Generation
5GNOW	Fifth Generation Non-Orthogonal Waveforms
ABG	Alpha Beta Gamma
AoA	Angle of Arrival
AoD	Angle of Departure
AP	Access Point
ARQ	Automatic Repeat Request
ASE	Application Programming Interface
BCCH	Broadcast Channel Configuration
BCH	Broadcast Channel
BER	Bit Error Rate
bps	Bits Per Second
BS	Base Station
BSC	Base Station Controller
CAPEX	Capital Expenditure
CCH	Control Channel
CDMA	Code Division Multiple Access
CFO	Carrier Frequency Offset
CIR	Address Resolution Protocol
CMT	Cosine Modulated Tone
CoMP	Coordinated Multi Point

CP	Cyclic Prefix
CSI	Channel State Information
DAS	Distributed Antenna Systems
DCCH	Dedicated Control Channel
DTCH	Dedicated Traffic Channel
eMLPP	Enhanced Multi Level Precedence and Preemption
eNB	Enhanced Node B
EPC	Evolved Packet Core
ETCS	European Train Control System
E-UTRAN	Evolved Universal Terrestrial Radio Access Network
EVM	Error Vector Magnitude
FBMC	Filter Band Multi-Carrier
FDMA	Frequency Division Multi Access
FFT	Fast Fourier Transform
FMT	Filtered Multi-Tone
FRA	Federal Railroad Administration
FSPL	Free Space Path Loss
GFDM	Generalized Frequency Division Multiplexing
GSM	Global Systems for Mobile Communications
GSM-R	GSM for Railways

HARQ	Hybrid Automatic Repeat Request
HSR	High-speed Railways
HSS	Home Subscriber Server
HST	High-speed Train
ICI	Inter Carrier Interference
IFFT	Inverse Fast Fourier Transform
IMT	International Mobile Telecommunications
IMT-A	IMT-Advanced
LOS	Line of Sight
LTE	Long Term Evolution
LTE-R	LTE for Railways
MAC-3FLCM	Multi Antenna Circular FIFO Fiber Fed Logical Cell Mapping
MBMS	Multimedia Broadcast Multicast Services
MCCH	Multicast Control Channel
MCH-C	Multicast Channel for C-plane
MEC	Moving Extended Cell
MFC	Moving Frequency Cell
MGMA	Multiple Group Multiple Antenna
MIMO	Multi Input Multi Antenna
MME	Mobility Management Entity
mmWave	Millimeter Wave
MTCH	Multicast Channel for C-plane

MU-MIMO	Multi User MIMO
NLOS	Non-Line of Sight
OBU	On Board Unit
OFDM	Orthogonal Frequency Division Multiplexing
OQAM	Orthogonal Quadrature Amplitude Modulation
PAPR	peak-to-average power ratio
PBCH	Physical Broadcast Channel
PCCH	Paging Control Channel
PCFICH	Physical Control Format Indicator Channel
PCRF	Policy and Charging Rules Function
PDN	Packet Data Network
PDP	Power Delay Profile
PHICH	Physical Hybrid Automatic Repeat Indicator Channel
PMCCCH	Physical Multicast Control Channel
PTC QoS	Positive Train Control Quality of Service
RADIATE	RADio over fiber as AnTenna Extender
RAMS	Reliability, Availability, Maintainability and Safety
RAU	Remote Antenna Unit

RMa	Rural Macro
RMS	Root Mean Square
RRC	Root Raised Cosine
RRM	Radio Resource Management
RSRP	Reference Signal Received Power
RSRQ	Reference Signal Strength Quality
RSSI	Received Signal Strength Indication
RTT	Round Trip Time
SDN	Software Defined Network
SGSN	Serving General Packet Radio Service
SGW	Serving Gateway
SINR	Signal to Interference plus Noise Ratio
SMT	Staggered Multi-Tone
SNR	Signal to Noise Ratio
STO	Symbol Time Offset
TTI	Time Transmission Interval
UCD	User Control plane Decoupling
UCDA	User Control plane Decoupling Architecture
UE	User Equipment
UIC	International Union of Railways
VBS	Voice Broadband Services
VGCS	Voice Group Call Services

WSSUS

Wide Sense Stationary Uncorrelated

Scattering

ZF

Zero Forcing

Chapter 1. INTRODUCTION TO HIGH-SPEED TRAIN COMMUNICATION CHANNELS

1.1. Importance of High-speed Train

High-speed Trains (HST) strategically becomes attractive as a mode of transportation compared to flights when the travel time is less than 2-3 hours. Almost 80% of the commuters consider HST for their daily commute due to commercial speed and comfort, frequency, accessibility, attractive door-to-door travel time, safety and reliability [1]. Normally a speed of of 300-350 km/hr is considered average commercial speed for the HST to be competitive against flights. Through extensive testing and innovation, it may reach a speed of 500 km/hr. In the Europe and Asia, railroads industry has been aggressive to deploy more number of HST corridors to serve passenger interests. The economic and environmental integrity, alongside future driven decision making of International Union of Railways (UIC) to manage the high-speed corridors, have already made HST a lucrative and futuristic transportation solution.

In 2015, UIC was targeting to adapt with higher commercial speed, new telecommunication technologies but in more environment friendly and energy efficient manners [2]. In addition, the means to increase passenger capacity have been explored as well as, infrastructure cost have been sought to highly optimize.

In the US, the interest over HST has not been overwhelming enough until but recently with California High-speed Railways. Before that, Amtrak has been a major service provider in northeast corridor in the US. The activities and interests are likely to grow with industrial venture of Hyperloop, where the train speed will reach an overwhelming 1000km/hr. The Northeast Corridor for Amtrak is also evolving towards

next phase with their new Acela fleets, which are able to provide a velocity of 180-220 Mph. However, the growing interest in high-speed ground transportation does not adequately reflect towards Positive Train Control (PTC) for a reliable communication specification lowering the communication latency. Therefore, as per UIC guidelines high-speed rail corridors will be highly customized, innovative and open for PTC integration with respect to technological ventures in communication, track and train construction. Our lab has been one of the partners of FRA to provide, assess and measure the high-speed passenger train communication channel scenario.

Safe operations of HSTs after a successful deployment completely rely on efficient signaling, train to track communications, train control and maintenance information acquisition, etc. They are called train control and signaling information. Efficient information flow of train control and signaling data between the control center and train makes the entire system reliable and working towards managing HST operations in large scale. However, the communication channels in train are responsible for providing passenger services including Wi-Fi and passenger support, ticketing and reservation information, marketing and advertising, ticket and access control and post-travel services. Maintaining communications in high-speed mobility is challenging, but managing seamless connection with guaranteed Quality-of-service (QoS) towards train-control services and offering on-board internet services to passengers with bandwidth extensive multimedia services, become highly challenging. Mobility induces additional challenges in a communication channel. The challenges introduced by high-speed mobility become hard to address as the channel bandwidth and frequency become higher to accommodate more number of multimedia services and users. Therefore, a thorough study of high-speed communication channels with respect to

recent advancement in radio access method is required. And, additional challenges related to adapting new radio access method should be addressed in a infrastructure friendly manner.

1.2. High-speed Train Communication Channel Scenario

HST wireless communication channels are often considered to be rural channel scenarios being fundamentally different than public land radio network. However, typical HST environment is affected by its surrounding environment, i.e, viaduct, tunnels, stations, cuttings, crossings, bridges, stations and combinations of these environments (grouped tunnels, tunnels and viaducts). These obstacles accumulate a deep fading in a rural channel model [3]. In addition to that, wind barriers, acoustic barriers, passing trains and arch grids add excess pathloss in the channel scenario [3]. These special scenarios are '*railway furniture*', which result in reflection or diffusion or scattering loss. The wireless channels in high-speed traffic are often considered to be Wide Sense Stationary Uncorrelated Scattering (WSSUS) channels accommodating vehicular channels. However, HST communication channel in turn shows rapidly time varying and non-stationary characteristics.

For most of the time, Line-of-Sight(LOS) component exists in HST channels and number of multi-paths, scatterers and shadowing are limited. However, this results in large multipath components and correlated scattering [3]. High mobility also introduces superimposed Doppler shift and spread in individual multipath components. Due to rapidly changing environments multipath components also suffer from fast variation. Therefore, channel and Doppler shift estimation becomes more challenging in HST channels. Moreover, due to high-speed mobility handover occurs faster than the usual mobility.

Based on physical environments wireless communication channels are segregated as urban, suburban, rural channel models. However, due to LOS, Non-Line of Sight (NLOS) channel variations cause rapid environmental changes in high-speed mobility. Based on these high-speed train environments, Bo Ai *et al.* partitioned them as scenes. These scenes based environment partition are shown in Table 1.1. Figure 1.1

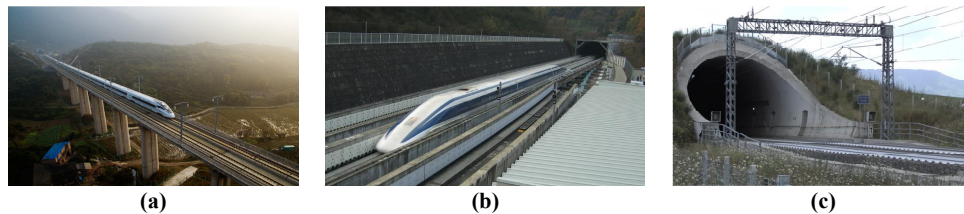


Figure 1.1: Different HST environment scenarios: (a) Viaduct, (b) Cutting, (c) Tunnel

shows different environmental scenarios in HST. The standardization bodies involved in high-speed train channel modelling do not consider specific high-speed train channel

Table 1.1: Scene Partition for HST Environments

Scenes	Definitions	Scenes	Definitions	Scenes	Definitions
S1	Viaduct	S5	Water-5a: River and lake areas	S9	Mountain-9a: Normal mountain
			Water-5b: Sea area		Mountain-9b: Far mountain
S2	Cutting	S6	Urban	S10	Desert
S3	Tunnel	S7	Suburban	S11	Combination scenario-11a: Tunnel group
					Combination scenario-11b: Cutting-group
S4	Station-4a (medium or small sized station)	S8	Rural	S12	In-carriage-12a: Relay transmission
	Station-4b (large station)				In-carriage-12b: Direct transmission
	Station-4c (Marshalling station and container depot)				

environments. Specifically, frequencies higher than 6GHz cannot be generalized with the standardized models [3-6]. For example, WINNER project group defined rural moving channel mentioned as D2a to model HST scenarios [4]. Even, in LTE HST channel models are considered to be non-fading channel model [6] with only one multipath component having Doppler shift. Special scenarios mentioned in Table 1.1

are largely ignored by standardization bodies, i.e., International Mobile Telecom (IMT), 3GPP, WINNER, etc. [3-6]. Considering next generation wireless systems being heterogenous, to support the need of passengers and high QoS requirement of train control channel, the models need to consider different frequency characteristics in time varying channels and HST specific environments.

1.2.1 Time Varying Channel

HST communication channels face time variability due to its high mobility. Considering a train changing its position, each signal propagation path changes correspondingly, and has corresponding effects on path delay and path gain. Figure 1.2 shows that a train moves by $\Delta \vec{d}$, from an old position to a new position. Then the angle between k -th ray and $\Delta \vec{d}$ (k -th incoming ray and direction of the train) is denoted as $\psi_k = \theta_k - \delta$. Where, $\delta = \angle \Delta \vec{d}$ and Angle-of-Arrival (AoA) of k -th path is θ_k .

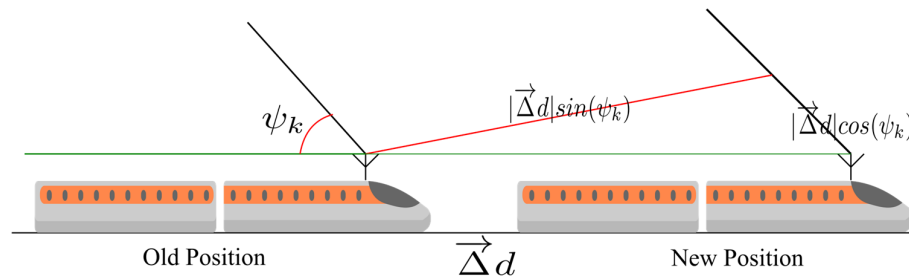


Figure 1.2: Train movement and simple ray tracing

Therefore, the length of k -th path increases by $|\Delta \vec{d}| \cos(\psi_k)$. The typical distance $|\Delta \vec{d}|$ depends on the train velocity and time-scale ΔT of interest.

- a) Path gain:** Path gain a_k decays inversely proportional to the square of length of path to the old position d_k as, $a_k \sim d_k^{-2}$, where $d_k = c\tau_k$. τ_k is the delay for the k -th path and changes at most $|\Delta \vec{d}|/c$, where, c is the speed of light. The

relative change in the path gain in HST communication channel is proportional to $\left(\frac{|\Delta\vec{d}|}{d_k}\right)^2$.

- b) Path Delay:** The relative change in delay is proportional to $\frac{|\Delta\vec{d}|}{d_k}$. The carrier frequency f_c multiplies the delay changes to produce phase shifts.
- c) Phase Changes:** The phase changes arise from the movement of the train to produce k -th path phase change as,

$$\Delta\phi_k = -\frac{2\pi f_c}{c} |\Delta\vec{d}| \cos(\psi_k) = -2\pi |\Delta\vec{d}| / \lambda_c \cos(\psi_k) \quad (1.1)$$

Where, $\lambda_c = \frac{c}{f_c}$ denotes the carrier wavelength. The phase changes are significant and leads to fast fading [7]. Table 1.2 shows the generic results for a

Table 1.2: Phase Change tracking for HST environment

Assuming $f_c = 2.5\text{GHz}$ and $\psi_k = 0$, $\Delta T = 1\text{ms}$			
v (m/s)	$ \Delta\vec{d} $ (m)	$\Delta\phi$ (degrees)	Comment
100	0.36	1080	Regular phase changes
200	0.72	2160	Medium
350	1.26	3780	High
500	1.8	5400	High
1000	3.6	10800	Very high

HST channel.

1.2.2 Large & Small Scaling Fading in HST

In large scale fading path loss and shadowing have been considered. For wireless network planning link budget computation, path loss and shadowing channel models are widely considered [8-9]. Shadow fading is mostly considered with a log-normal distribution and in a typical path loss model as (1.2),

$$PL(d) = A + 10n \log_{10}(d) + X_{\sigma} \quad (1.2)$$

Path loss exponents n are calculated for different environment or physical scenarios where d is the distance between transmit and receive units in meters (m) and A is the intercept. The Shadow fading for different environment can be seen in Figure 1.3 and mostly varies from 2 – 6, where the highest shadow fading variance can be found in Rural macro cell areas. Whereas, indoor and viaduct scenario show lower shadow

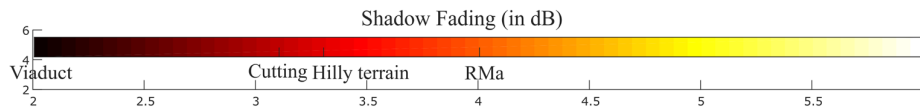


Figure 1.3: Shadow fading in different HST environment scenarios fading variance.

Small scale modeling approaches can be modeled with deterministic and stochastic channel models based on ray-tracing, Markov-chains, etc. Authors have addressed scenario based small scale fading in [3, 8-10] based on time-varying nonstationary channel characteristics.

1.2.3 Nonstationarity of The HST Communication Channel

The channel statistics, multi path components change rapidly over a short period of time as the train travel a large distance over a large region, introducing nonstationarity in HST communication channels. Nonstationarity affects the Bit Error Rate (BER) of the channel significantly. Most of the time, large scale fading (path loss, delay spread) have been the modus operandi in academia. But small scale fading have been largely ignored. In both, WINNER II Rural Macro (RMa) or D2a and IMT-Advanced channel moving network models, the speed of the train can be considered as 350 km/h. However, in a physical HST testing scenario, maximum time over the Wide-

Sense Stationary (WSS) channel condition being considerably lower than both the channel models satisfies the inadequacy of the channel models [3].

But the site specific and frequency dependent models cannot be generalized for future HST networks. Nonstationary models should consider time-variant model parameters: angular parameters, Doppler frequency, Ricean K factors and the distance between Tx and Rx based on the scatterers. The fast-varying effect of the channel as it passes through different channel environments at very short interval, influences receiver design. Due to LOS component existence in the channel, nonstationary LOS Multiple Input Multiple Output (MIMO) channel model has gained popularity to increase throughput. The time-varying small scale fading parameters, affects LOS MIMO design. Due to correlated multipath mentioned in [3, 11], the channel is trivially rank-deficient. Therefore, antenna elements should be designed to maintain orthogonality. The channel response matrix of LOS MIMO can be denoted as (1.3),

$$H = \sqrt{\frac{K}{K+1}} H_{LOS} + \sqrt{\frac{1}{K+1}} H_{NLOS} \quad (1.3)$$

Where, H denotes the LOS MIMO channel response matrix, H_{LOS} and H_{NLOS} are the *LOS* and *NLOS* channel coefficients respectively, K is the Ricean K -factor in linear scale.

1.3. Challenges in HST Communication

As it is previously discussed, channel estimation in high-speed train environment is highly challenging due to large and small-scale fading introduced by high mobility, fast-changing environment and stringent QoS requirement in train control plane. Recent HST communication uses Multi-Input Multi-Output (MIMO)

technologies, beamforming, Orthogonal Frequency Division Multiplexing (OFDM) and other methods to provide optimal services to passengers. However, each one of them has their limitation considering high mobility, fast variation and nonstationarity in channels. Thus, following discusses further challenges involved in channel estimation.

1.3.1 Doppler Shift and Spread

Doppler shift and spread have been considered to be part of time-variant channel characteristics. Considering a train moving at a constant velocity v , the distance $|\Delta \vec{d}| = vt$.

Consequently, the k -th path phase change can be considered as from (1.4),

$$\Delta \phi_k(t) = -\frac{2\pi v}{\lambda_c} \cos(\psi_k) t = -\frac{2\pi v}{c} f_c \cos(\psi_k) t \quad (1.4)$$

Hence, the signal experiences a frequency shift of $f_{d,k} = \frac{v}{c} \cdot f_c \cos(\psi_k)$. The frequency shift is called Doppler shift. Each signal experiences different Doppler shift due to AoA being different. Several Doppler shifts along the path create Doppler Spectrum. Doppler shifts are trackable in HSR environment due to constant speed of train along the cellular sites. Doppler spectrum attributes to range of frequency shifts ranging from $-f_d$ to f_d , induced by time-varying channel, where $f_d = \frac{v}{c} \cdot f_c$ being the Doppler spread. Doppler spread leads to loss of Signal-to-Interference-Plus-Noise-Ratio (SINR) and obfuscates carrier recovery and synchronization. Doppler spread is also a concern of OFDM system as it can corrupt the orthogonality of subcarriers [3, 12-16].

In a HST, the distance between User Equipment (UE) and eNB changes rapidly. Therefore, Doppler shift affects both downlink and uplink signals. Due to constant velocity the train, only change in the direction between incoming ray and train

contributes to Doppler spread. In the LTE standards, open space and tunnel model have been considered [3]. In a basic 3GPP non-fading model, Doppler shift at specific time is considered as, $f_{d,k}(t)$ with direction specified by (1.5)[6],

$$\cos(\psi_k(t)) = \begin{cases} \frac{\frac{D_s}{2} - vt}{\left(\sqrt{D_{min}^2 + \left(\frac{D_s}{2} - vt\right)^2}\right)}, 0 \leq t \leq \frac{D_s}{v} \\ \frac{-1.5D_s + vt}{\sqrt{D_{min}^2 + (1 - .5D_s + vt)^2}}, \frac{D_s}{v} < t \leq \frac{2D_s}{v} \\ \cos\psi\left(t \left\lfloor \frac{2D_s}{v} \right\rfloor\right), t > \frac{2D_s}{v} \end{cases} \quad (1.5)$$

Figure 1.4, shows the Doppler shift varies with carrier frequency, velocity, distance from the BS, etc where D_{min} is the train to track distance and $\frac{D_s}{2}$ being initial starting point. Considering a mmWave frequency of 28GHz Figure 1.4 have been simulated for two respective velocities, $v = 300$ km/h and $v = 1000$ km/h and shown

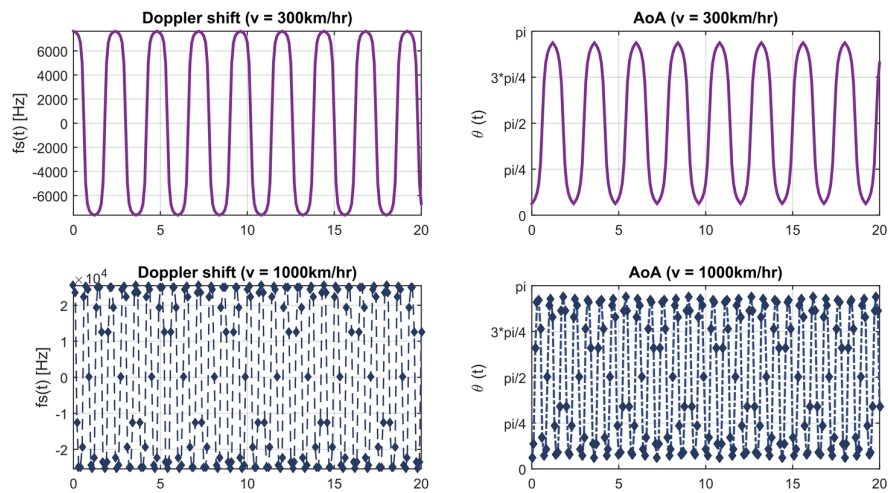


Figure 1.4: Doppler shift for $f_c = 28$ GHz and $v = 300$ and 1000 km/hr

that for velocity higher than 1000km/h, the Doppler shift reaches 20 KHz, which is greater than max cyclic prefix of LTE.

1.3.2 Inter-Carrier Interference

In regular communication, a time invariant channel there is no interference between adjacent subcarriers because of the orthogonality, which is assured due to the length of cyclic prefix (CP) being greater than the channel order [12]. The transmitted signals can be recovered simply inverting the channel on each subcarrier. In HST environment, Doppler shift changes the bandwidth by some factors and eventually destroys or degrades orthogonality between subcarriers. It results in a signal spread in the received signal from one subcarrier to another. With increasing Doppler effects, the spread increases from spreads to the orthogonal subcarrier. The phenomenon is called Inter-Carrier Interference (ICI). The carrier Frequency Offset between transmitter and receiver oscillator can incur same effects as Doppler shift and ICI. If the level of ICI is high, the leakage or interference from adjacent subcarrier make it impossible for transmitting signal to recover. Eventually, the receiver design becomes complex with higher frequencies, higher bandwidth, and more number of subcarriers.

1.3.3 Fast Handover

A moving unit moves one coverage area to another coverage area of base stations. These movement contributes to successive reconnections and thus called handover to next base station. A train moving linearly at high-speed changes connecting base stations rapidly. The rate of handover thus increases drastically. Depending on frequency, base station coverage and speed of train the number of handover changes. Traditional cellular network with a large coverage area introduces handover every 10-20s and in recent LTE systems the handover may occur every 1-5s. Thus, handover may lead to packet loss and reordering. In a general hard handover scheme in HSR, when a train moves to an overlapping region of cell i , eNB_i initiates the handover

based on Received Signal Strength Indication (RSSI), Reference Signal Received Power (RSRP) or Reference Signal Strength Quality (RSRQ) information from the train and Radio Resource Management (RRM) [17]. With the handover trigger, the train connects to target BS, and eNB_j moves into the j -th cell. Obviously, due to constant reconnections, after disconnecting from previous BS, it creates additional signal and temporal overhead, which is shown in Figure 1.5 [17]. Therefore, adapting to new

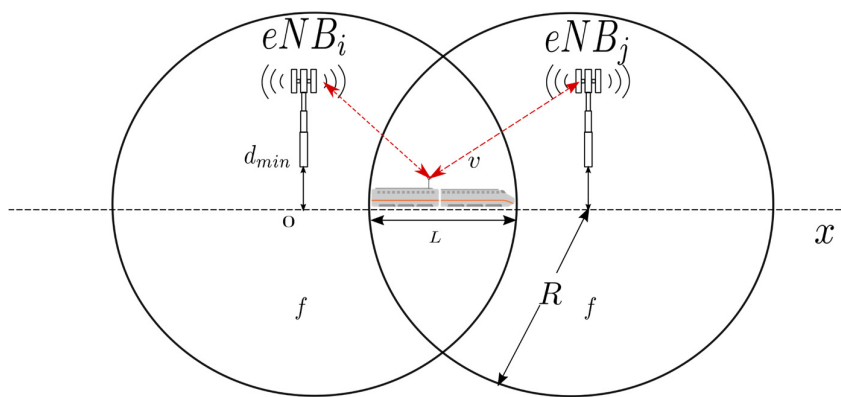


Figure 1.5: Hard handover scenario

cellular technologies leads to minimizing number of handovers and maximizing handover success probability.

1.3.4 Delay Spread

Delay spread is the delay dispersion brought by the multi-path components to wireless channel responses that leads to frequency selective fading. To analyze delay spread, relative parameters are maximum excess delay and Root Mean Square (RMS) delay spread. Maximum excess delay is defined as, $\tau_{max} = \tau_x - \tau_l$, where it is a time delay difference between the last arrival signal and first arrival signal. τ_l is the first arriving wave delay and τ_x is the maximum delay of the last signal whose power was above the noise floor. The RMS delay spread can be defined by the square root of the second central moment of the Power delay Profile (PDP) as,

$$\sigma_{\tau} = \sqrt{\frac{\sum_l P(\tau_l)(\tau_l - \bar{\tau})^2}{\sum_l P(\tau_l)}} \quad (1.6)$$

Where $P(\tau_l)$ is the power of the l -th path ($l = 1, \dots, L$) and τ_l is the propagation delay of the l -th path. $\bar{\tau}$ is the first moment of the instantaneous PDP and can be computed as,

$$\bar{\tau} = \frac{\sum_l P(\tau_l)\tau_l}{\sum_l P(\tau_l)} \quad (1.7)$$

Therefore, delay spread is dependent on environmental changes. Environments where cuttings exists, rich multiple reflections leads to larger delay spreading. A hilly terrain scenario has been shown in [18]. It shows that, in tunnels, before entering and after leaving the tunnel delay spread becomes exceptionally large. Therefore, it is important in HST channel scenario to study delay spread thoroughly.

1.3.5 Linear Coverage

The special scenario of HSR and BS deployment along the track make a highly predictable architecture in HSR environment. The BS antennas being directional, their main lobes can be directed towards track and BS are deployed linearly. Therefore, with known location of the train, efficient beamforming algorithms can be written [15].

However, the scenario is particularly different than normal hexagonal or stochastic cellular diagrams. Due to shadow fading some locations in the linear coverage will receive signal below a particular threshold [15]. Therefore, calculation of link budget is different in HSR scenario.

1.3.6 Sparse Multipath

In open space models (viaduct, rural, etc.), there are very few scatterers. The linear coverage areas also decrease the number of scatterers, directly seen by the transmitters and receivers. So, most of the time LOS path is considered. Sparse multipath channels are sparsely distributed resolvable paths in the angle-delay-Doppler domain [3, 15]. As MIMO is supported in recent communication systems, the performance of multi antenna solutions depend on spatial diversity and multiplexing. In an open space, due to strong LOS component strong correlation between the signals of two antennas reduce diversity and multiplexing gain. Therefore, in sparse environments, reconfigurable antenna array may significantly improve capacity [3, 15].

1.3.7 Train Car Related Issues

A high-speed train can be 200m long and in China it is 400m to support increasing demand and passenger capacity [3, 15]. Trains are mostly made of metal. The trains themselves act as scatterer and reflector, and increase delay spread. Considering an evolution towards 5G and mmWave frequencies, large metal roof of the train will significantly increase reflections and scattering near antennas and influence the patterns. The side and main lobes of the antennas are highly influenced by the on-roof metal surface, which incurs design issues alongside fabrication problems. High penetration loss due metal body and glass windows will also affect SNR of the signal. Due to separate loss characteristics mmWave propagation characteristics inside train is required for each in-train network deployment in different region.

1.4. Envisioning Next Generation HST & HST Wireless Communication for High-speed Ground Mobility

The next generation wireless communication scheme involves high capacity and very low latency. The fifth-generation wireless communication covers a lot of ground related to different wireless environment and provide the best possible quality of service to accommodate the next generation applications. The applications involve tactile internet, augmented reality, virtual reality, Device-to-Device (D2D) internet and multimedia communication to evolving and bandwidth intensive broadband internet. The increasing number of internet connected devices also puts a load on the available network. Following the trend, HST network will face changing characteristics and highly bandwidth intensive passenger and train control traffic in near future, which cannot be directly supported by the methods available without a massive CAPEX. The mobile environment includes a very challenging barrier to communication, with future physical layer changes, i.e., massive MIMO, mmWave, beamforming or integrating them altogether will incur additional complexity for low latency communication. However, the trends all connect towards more number of BS deployment. Therefore, with changing radio access technologies, the dense deployment should follow the mobility in a close connected manner, so that in each RTT there is a BS for transmitting and receiving.

Chapter 2. COMMUNICATION METHODOLOGIES IN HST

This chapter will provide a brief overview of the involved communication methodologies in recent HST from evolution of GSM for Railways to LTE for Railways (LTE-R), Distributed Antenna System, Remote Antenna Units, Moving Extended Cells (MEC), Femto cells and Radio over Fiber (RoF). Where, the first two are radio access methods and rests are architectures to utilize the cellular capability at high-speed.

2.1. GSM-R to LTE-R

The section describes a comparative overview of two major radio access methods in railways and their corresponding advantages and disadvantages.

2.1.1. GSM-R

Standard HST communication system relies on voice and data communications for safety and control operation. Earlier the Global System for mobile Communications-Railways (GSM-R) has proven to reliably operate over narrowband bandwidth limited applications [14, 15] for railway specific applications. The usual frequency bands are 873-876 MHz for uplink and 918-921 MHz for downlink with 7-15 km between neighboring BSs. GSM-R have been used for the European Train Control Station (ETCS) for voice and data carrier services.

2.1.2. GSM-R Services

In ETCS first level or ETCS-1, GSM-R has been used for only voice services. ETCS-2 and ETCS-2 used GSM-R for data transmissions. However, even if GSM-R

can support a speed of 350 km/hr, for call drops or loss, train has to automatically reduce speed below 300 km/hr. GSM-R in HST has to support following services reported by [15],

- a) **Voice Group Call Service (VGCS):** It is group call service between train and BS, trackside workers or station staffs.
- b) **Voice Broadcast Service (VBS):** In this service train can broadcast to other trains or BS in a certain area, where an initiator can start the service and others can join the call and listen.
- c) **Enhanced Multi Level Precedence and Preemption (eMLPP):** It defines the priority among calls to maintain QoS to high priority services.
- d) **Shunting Mode:** A group call to the staffs involved with shunting operation.
- e) **Functional Addressing:** A train is addressed by a functionally addressed number.
- f) **Location-Independent Addressing:** As the train moves through different location, calls from train can be addressed completely location based.

Eventually, the lifetime of GSM-R has been in its final stage due to end of vendor support, integration of more number of critical train services and lack of extension of support towards broadband access.

2.1.3. LTE-R

LTE-R is not a substitution of GSM-R. The voracious evolution of LTE has made it a potential candidate towards future existence in different applications. In high-speed railways, LTE-R not only can support critical services, but also provide other information and communication services to passengers and train control plane. LTE-R

is considered standalone radio access method for railways now due to its fulfillment of railways requirement of Reliability, Availability, Maintainability, and Safety (RAMS). In a typical high-speed scenario spectrum harmonization, end-to-end QoS requirements, reliable system performance, backward and forward compatibility, are considered to be critical for a radio access method [14, 15]. It is now also clear the LTE evolution towards 5G can support a massive Gigabits capacity to cater future non-critical passenger multimedia service needs [1, 19]. Thus, LTE has some advantages over GSM-R based on capacity and capabilities. LTE being packet-switched network, data communications are better suitable with LTE based network. LTE has efficient call set up time and reduced packet delay agreeing to ETCS message requirements [14, 15]. It also provides standardized interworking capabilities with GSM. There are many different bands, which are used in different continents. Figure 2.1 shows the bands

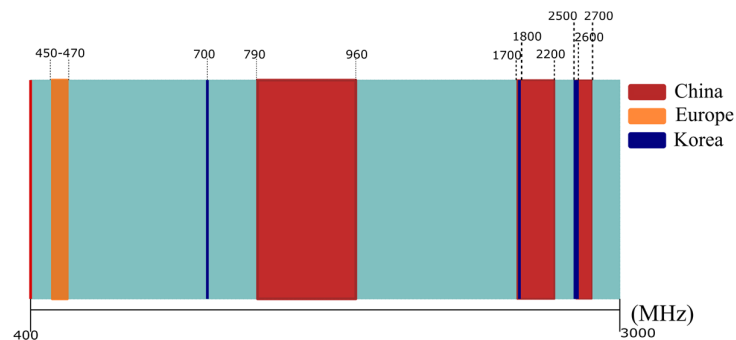


Figure 2.1: LTE-R Frequency allocation in different continents

involved in LTE-R (China, Europe, and Korea) and Table 2.1 shows the comparative overview of radio access methods. It is to be noted that LTE-R is configured for reliability more than capacity. Therefore, capacity is highly normalized for a better performance.

Standard LTE includes Evolved Packet Core (EPC) and a radio access network Evolved Universal Terrestrial Radio Access Network (E-UTRAN). The Internet

Protocol based EPC can support seamless handovers in both voice and data transmissions. LTE-R is derived from LTE and comprises of radio access systems to

Table 2.1: Comparison among radio access methods [15]

Parameter	GSM-R	LTE	LTE-R
Frequency	Uplink: 876-880 MHz Downlink: 921-925 MHz	800 MHz, 1.8 GHz, 2.6 GHz	450 MHz, 800 MHz, 1.4 GHz, 1.8 GHz
Bandwidth	0.2 MHz	1.4-20 MHz	1.4-20 MHz
Modulation	GMSK	QPSK/M- QAM/OFDM	QPSK/16-QAM
Cell range	9 km	1-5km	4-12 km
Cell configuration	Single sector	Multisector	Single sector
Peak data rate, downlink/uplink	172/172 Kbps	50/100 Mbps	10/50 Mbps
Peak spectral efficiency	0.33 bps/Hz	16.32 bps/Hz	2.55 bps/Hz
Data transmission	Requires voice call set up	Packet switching	Packet switching (UDP packets)
Packet retransmission	Serial, circuit switched	Yes (IP packets)	Reduced (UDP packets)
MIMO	No	$2 \times 2, 4 \times 4$	2×2
Mobility	Max 500 km/h	Max. 350 km/h	Max. 500 km/h
Handover success rate	$\geq 99.5\%$	$\geq 99.5\%$	$\geq 99.5\%$
Handover procedure	Hard	Hard/soft	Soft: seamless
All IP (native)	No	Yes	Yes

exchange wireless signals with On-Board Units (OBU) on trains [15]. A backward compatible LTE-R architecture is shown in Figure 2.2. To consider services of LTE to provide to HST, GSM-R services should be extended alongside LTE-R specific services as explained in the next section.

2.1.4. LTE-R Services

LTE-R may provide services that are better than traditional GSM-R and can coexist with GSM-R, which are [14, 15]-

- a) **Information Transmission of Control Systems:** LTE-R can achieve a real-time transmission of control information with a transmission delay of < 50 ms, which is compatible with ETCS-3.

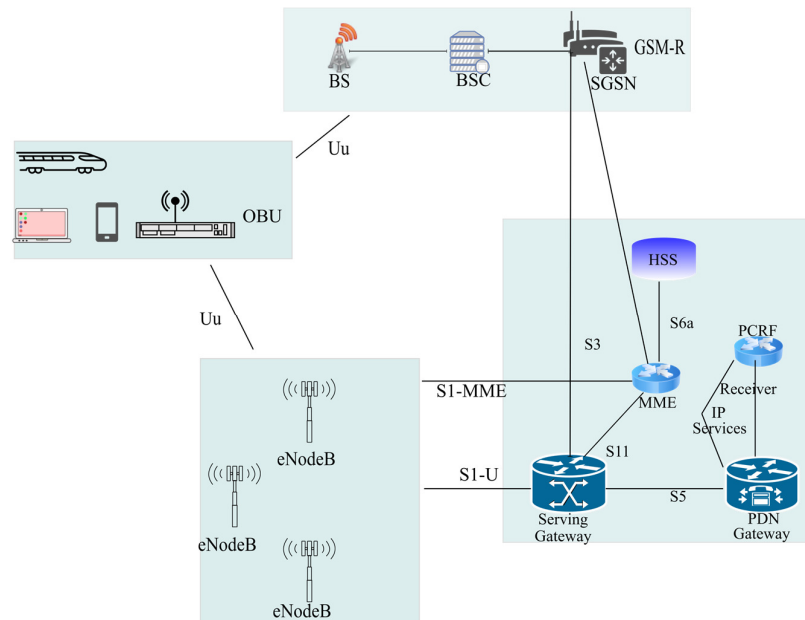


Figure 2.2: LTE-R architecture with backwards GSM-R compatibility

- b) **Real-Time monitoring:** Real-time monitoring includes video monitoring of cabin, car joints, track conditions with temperature and fault detection. The monitoring information are shared with the control center with a minimal $< 300\text{ms}$ delay.
- c) **Train Multimedia Dispatching:** LTE-R can transmit full dispatching information including text, voice, image, videos, etc. to yards and other trains.
- d) **Railway Emergency Services:** During natural disasters, accidents, derailments and other emergencies, prompt information transfer is necessary. LTE-R can use railway private network for faster response with a delay of $< 100\text{ms}$ compared to GSM-R.
- e) **Railway Internet-of-Things (IoT):** As UIC is considering more optimized rolling stock tracking [15, 19], LTE based Machine-to-Machine (M2M) communication can integrate real-time query and tracking of trains and goods

carried by trains. The trackside infrastructure and maintenance would also gain the advantage of seamless connection and automated inspection and operation. Finally, LTE-R is not devoid of the challenges involved in HSR communication. It faces the same mobility and nonstationarity related challenges, as the traditional GSM-R has been facing. However, there are many design tweaks specifically adapted in LTE-R for accommodating ICI, delay spread, Doppler spread, etc. [6]. 3GPP has been considering HST channel models as a part of LTE specification after Release 9 [6, 19]. LTE is being deployed from 400MHz to 2.7GHz. However, for simulation purposes Doppler spread of 555Hz can be considered for $f_c = 2GHz$ in HST scenario at $v = 300km/hr$. Subcarrier spacing in LTE/LTE-A is defined as $\Delta f = 15kHz$. Most of the LTE deployments worldwide use a subcarrier spacing of 15kHz resulting in 3 to 6 OFDM symbols respectively for Extended Cyclic Prefix. With a given subcarrier frequency design criteria of 15kHz an ICI through, Doppler shift can be ignored upto 350km/h [20]. However, the orthogonality is assumed through that the transmitter and receiver both are using same frequency. If there is a frequency offset introduced similar to Doppler effects, orthogonality and the effects of ICI can be observed. In mmWave frequency, phase noise adds additional error and measurement anomaly [20].

2.2. Architecture Considerations

There have been multitude of research selecting radio access methods and how are they considered to be potential technology for HST communication. However, the challenges involved in High-speed Railways can be addressed with efficient channel estimation and newer architecture or deployment consideration. There are architectures proposed involving Radio over Fiber (RoF) and Moving Extended Cell (MEC) with Distributed Antenna System (DAS), Remote Antenna Units (RAU), User & Control

Plane Decoupling (UCD), Coordinated MultiPoint (CoMP), femto cells, and multiple antenna. The architecture consideration can be divided into two groups: cellular and antenna based HSR communication enhancer and expander systems.

2.2.1. Radio over Fiber (RoF)

Lannoo *et al.* first proposed RoF for HST to provide broadband internet access to passengers (5 Mb/s/user) with sufficient QoS according to railways standards. According to their study, they argued that an aggregated capacity could be of 750Mb/s assuming there would be 750-1000 passengers in train within 2012 and the capacity requirement following the trend. In 2017, the standard user requirement has risen to 20-50Mbps, whereas 3GPP claims it to be in 1Gbps within 2020. Therefore, the aggregated capacity requirement for broadband access may reach up to 5-50Gbps. Considering extended and normal Cyclic Prefix (CP) in LTE for different environmental scenario as discussed in 2.1.3, it can support more than 25.1-59.8Mbps per user in an ideal case where packet drops and BER due to high-speed are minimal [20]. In a high-speed scenario, generally on an average LTE can only achieve 4-10Mbps [3, 15], for guaranteed reliability.

2.2.1.1 Access Network

The high bandwidth requirement of broadband access can only be realized with higher frequencies namely in microwave (300 MHz-300 GHz). The mmWave frequencies (30-300 GHz) are the most suitable wireless candidates. However, atmospheric attenuation and large penetration loss make it a challenge to use them as operational frequencies for HST [22]. The smaller cells namely pico to micro cells (100-500m) with highly dense deployments make good wireless access solutions. The authors considered 60 GHz frequencies to be a potential solution for future

communication network. However, we know due to severe attenuation even in indoor condition 60 GHz based 802.11ad could not be a potential candidate for next generation 5G networks.

A huge number of BS deployment is also inevitable, which is not an acceptable solution to railways. Thus, the RoF network is a fiber-based network solution to avoid potential delay shown in Figure 2.3. It is a fiber-based distributed antenna network. The

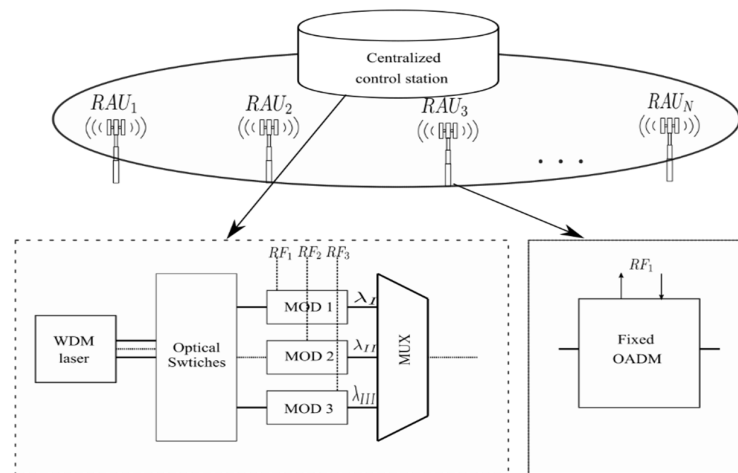


Figure 2.3: RoF ring distributed and WDM optical switched network [21]

goal of a RoF system is to share the complicated signal processing function namely: modulation/demodulation, multiplexing, synchronization, etc. from BS to linearly deployed RAUs in a BS coverage area. In Figure 2.3, optically ring distributed RAUs are located along the rail tracks and supervised by centralized control station involving BS. During communication, modulated data traffic at radio frequency namely in microwave to mmWave frequencies and are converted into optical signal and transmitted to RAU from control station through optical fiber [21]. The linearly deployed RAUs are the only one communicating with the train antenna due to fast switching among the RAUs through optical links. This leads to extension of MEC concept.

2.2.1.2 Moving Extended Cell

The concept of MEC came from physically moving cell which was proposed for highly mobile vehicular scenario [23]. The advantage of having physically moving cell is in minimizing the relative velocity. The architecture is shown in Figure 2.4. However, the Capital Expenditure (CAPEX) required to mechanically design a system

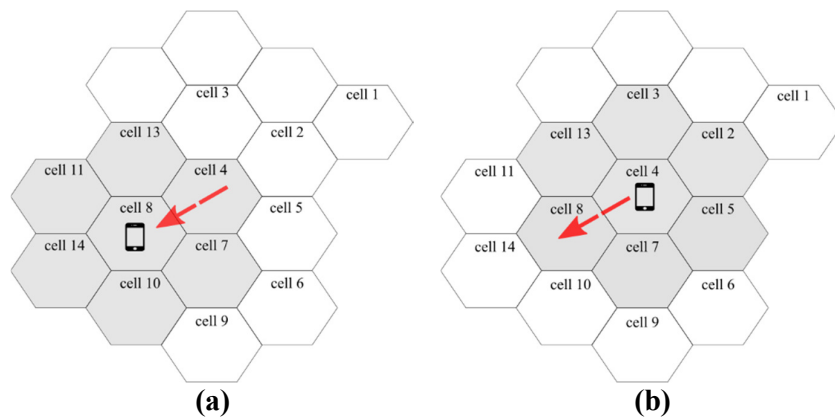


Figure 2.4: Moving Extended Cell Concept

that moves with the tracks, can be huge. The futurism involved in this method is novel but installing and maintaining two moving architecture is hard. Therefore, the concept of MEC is extended with DAS by the researchers from train with on-roof antennas and trackside RAU.

2.2.1.3 Moving Frequency Cell Concept

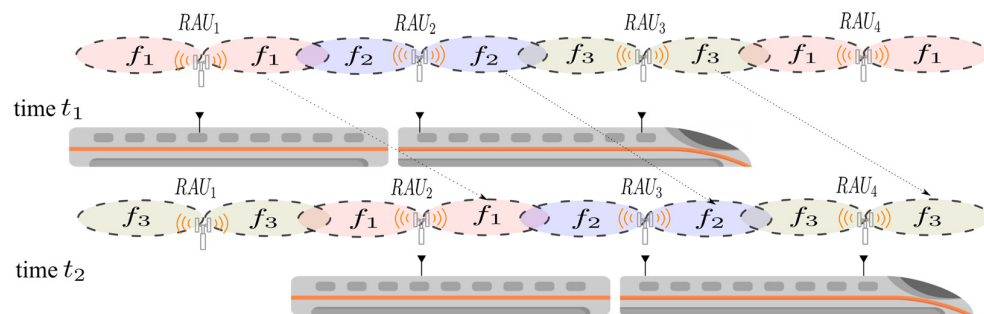


Figure 2.5: Moving Frequency Cell Concept [24]

The MFC is introduced by [24] to change the frequencies with the RAUs involved in communication along the movement of train. Therefore, each RAU cell will have a separate frequency assigned to it. In Figure 2.5 it is shown that RAU_1 , RAU_2 , RAU_3 and RAU_4 will have frequencies f_1 , f_2 , f_3 and f_4 respectively. In MFC, the moving frequencies are mapped with the on-roof antennas with optical switching among RAUs instead of handovers. The order of time is in ns or μs .

2.2.1.4. Optical Switching

Implementing RoF in a high-speed mobility environment a fast-optical switching architecture for making moving cells a reality. The proposed architecture in [21], utilizes a ring topology with single fiber covering all the RAUs in a control station region and switching between RAUs with Wavelength Division Multiplexing (WDM). As the wavelength is fixed, it is easy to switch output from a BS to RAU. According to Figure 2.3, the moving cells are implemented through switching optical switches. A fixed wavelength is terminated in each RAU having Optical Add Drop Multiplier (OADM) with WDM laser. WDM laser sends a light beam, which is sent through the fiber to an optical switch and with appropriate modulation at different wavelength for specific output port. In Figure 2.3, due to $m = 3$, the output order is λ_I , λ_{II} , λ_{III} . If λ_I is modulated with RF_1 , it is then multiplexed and transmitted to the right RAU. The RAU can then transmit the information to RF_1 , which is equipped with OADM.

2.2.1.4. Distributed Antenna and Remote Antenna Units

In a DAS, multiple RAUs are installed along the tracks in BS coverage to mimic the train movement or significantly drop channel variation with receiving signal at each Round Trip Time (RTT). Mostly, the RoF lines are deployed in tunnels and subways

when there is no direct LOS from BS or satellites. Chow *et al.* showed a WiMAX based RoF in Taiwan HSR with field trials [25]. As mentioned before, DAS are connected with optical links separated for uplinks and downlinks, which carry different modulated signals. The RAUs are responsible only for communicating with the train antenna in each RTT. To provide an example, a typical HST network may need 7 BS to cover 18 km area. Assuming, the train moves at 300 km/h, there will be 6 consecutive fast handovers within 316 seconds [25]. However, putting fiber connected RAUs within same region remove handovers entirely. The handovers between RAUs occur differently than between BSs,

- a) The process of handover relies on completely transferring control and data channel by evaluating received channel measurements (signal power, RSSI, etc.) to the next BS. Control station must decide the next BS, based on the measurements. The new BS has to initiate the handover through the previous BS to connect with the train [17, 25]. The connection is thus established through lower layer connection and handover bursts sent from the train.
- b) However, the RAUs are connected in same BS, so even if there is a handover between RAUs, the BS remains same after and before the handover. The radio channels in the communication is also same throughout the connection. Thus, there is no need of additional switching in lower layers. No additional synchronization among RAUs is also needed for shift in radio channels and preparing new BS.
- c) In a WiMAX channel of 802.16e, the TTG frame is $105\mu s$, which contributes to RTT (9km roundtrip over single mode optical mode optical fiber) [25]. The delay did not include switching and electrical conversion

delay and the theoretical maximum of distance between the BS in WiMAX RoF DAS is 18 km for utilizing handover for next BS.

The cell planning through RAUs are cost effective and provides the best handoff situation in HST network. Therefore, there are vendors who provides HST communications solutions based on RoF.

2.2.2. Small Cells

The small cells are coverage area of high frequency BS. Due to high frequency, the path loss of the signal is more and leads to smaller coverage area. According to frequency, the small cells can be called micro, femto and pico cells. The mobility in network often addressed by small cells to extend the range of in-train networks. The wireless network performance often suffers in in-train networks due to penetration loss. Therefore, a network architecture is designed with Mobile Relays (MR) inside the vehicles to which User Equipment (UE) connect to MRs, instead of directly connecting to macro BS. The MR based architecture can also be used in a tunnel or subway environment where the direct LOS is not present. Small cells along with indoor and outdoor antennas can provide a reliable communication for HST network, which is shown in Figure 2.6 and have been shown interest recently [26, 27]. In an in-train small cell architecture MR antennas are placed outside the carriage to communicate with the

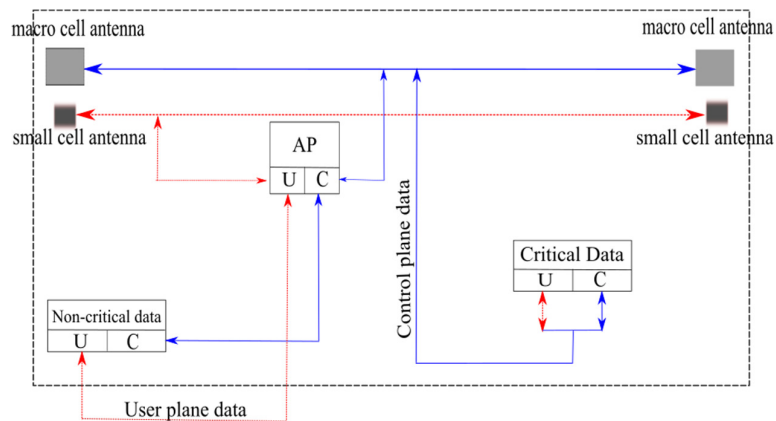


Figure 2.6: Small cell based network

BS. However, there will be severe Doppler shift and spread affecting uplink/downlink transmission. To avoid the challenges, MIMO and sophisticated beamforming can be used. However, that does not reduce the number of handovers and fast handovers involved in the communication [26, 27].

The deployment of MR in in-train network provides an opportunity towards building a heterogeneous architecture with LTE-A wireless backhaul and Wi-Fi front haul towards passengers for high-speed internet access. There are multiple avenues of research based on heterogeneous network with macro and small cells in HST which are surveyed in detail in [19].

The in-train small cell network is accessed by the UE with indoor antennas and outdoor antennas present a multi egress network [28]. Most of multi egress network exploits Mobile Access Router (MAR) architecture to integrate multiple access technologies to provide better link quality to UEs. However, detailed architecture providing control and data signaling is complex to design with routing optimization and Internet Protocol (IP) mobility issues [28]. Handover latency and buffer management in the network to provide seamless handover solving packet loss problem in the network, also remain challenging with evolved and more complex network

architectures like separation of user and control plane traffic with multiple access technologies, planes or frames.

2.2.3. Coordinated MultiPoint (CoMP)

Luo *et al.* introduced CoMP soft handover scheme in LTE-R communication systems [17]. The general hard handover scheme integrated in LTE provided very long delay in handover and a handover failures in overlapping area due to high-speed of the trains. CoMP basically permits two spatially separated BSs to simultaneously transmit and receive data from a UE, which significantly improves the spectral efficiency and inter-cell interference [17]. In his paper, Luo mentioned that with OFDM in LTE, Inter-cell Interference is the main source of interference [17].

The overall architecture can be described in Figure 2.7. The Handover happens when the train completely enters in overlapping region. However, both the antenna at

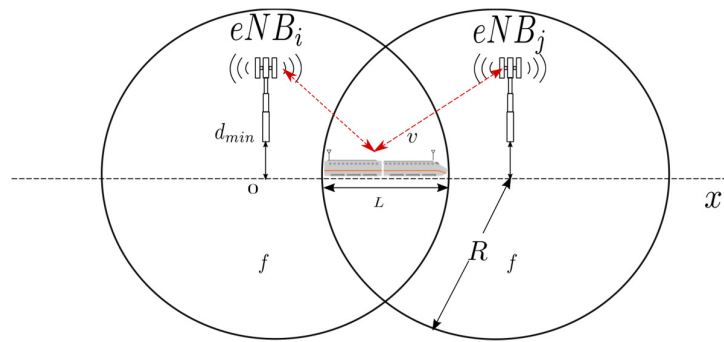


Figure 2.7: CoMP architecture [17]

tail and head are connected to eNB_i and eNB_j respectively. Both the eNB s are cooperative in nature, but, the measurement information is only sent to eNB_i . The handover occurs with the measurement information received by eNB_i and RRM information received by target eNB_j [17]. The handover is triggered when the signal strength of eNB_j is higher than eNB_i .

2.2.4 User and Control Plane Decoupling Architecture (UCDA)

User and Control Plane decoupling of LTE-B architecture was first proposed by [29], to increase spectral efficiency and achieving a 1000-fold increase in capacity with a similar heterogeneous architecture. An architecture with macro and small cells to extend coverage of macro cells and a basic enhancement of spectral efficiency can be modified with UCDA. In this architecture, the network becomes completely dependent on macro cell assistance. The control signaling which creates significant overhead due to number of small cell increasing and seamless connection requirement due to small cell handovers or connection through small cells, can be completely transferred to the macro cells. Whereas, small cells only carry the user data plane and mitigates the signaling overhead. In an HST environment, the similar concept is introduced which is shown in Figure 2.8. In HST environment to achieve a better reliability, train control

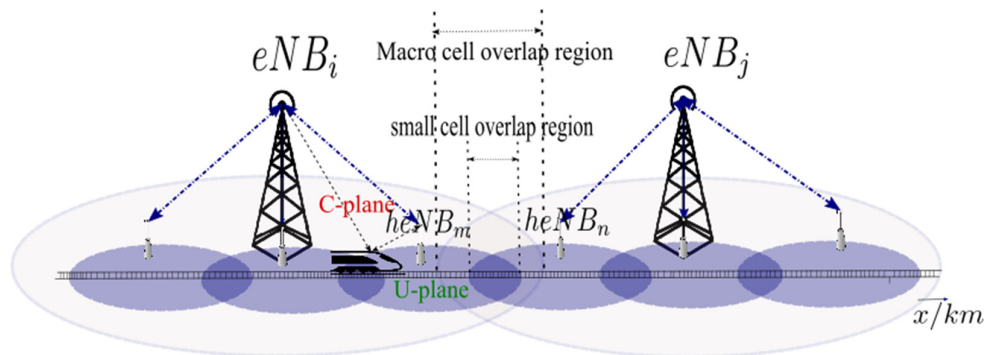


Figure 2.8: Conventional UCDA

data is integrated with passenger control plane to achieve HST-UCDA control plane. The user data can be accommodated in the user plane similarly to conventional architecture. The goal of this architecture proposed by [30], is to attain a reliability even using massive number of small cells under macro cell supervision. The small cells will

cater the future bandwidth need of the trains whereas macro cells will provide the desired reliability in the network.

2.2.5 On-Roof Antennas and RADIATE

There are many architecture researched by the academia for HST environment, i.e., CoMP [17], dual antenna handover [31], bi-casting or dual-link handover [32], Multiple Group Multiple Antenna (MGMA) Scheme [33]. The main concept behind all the architectures is using multiple on-roof antennas on train. Including femto cells, access points and mobile relays the network can be extended as in-train network. Most of the network architecture depends on in-train or backhaul fiber optics, which makes the scope being distributed antenna systems on-train. The best example of minimized latency train-to-ground network on-train is through RADio over fiber as AnTenna Extender (RADIATE) [34]. RADIATE depends on reducing Doppler shift due to train mobility over RTT. Han *et al.* suggested to deploy antennas on train as in Figure 2.9

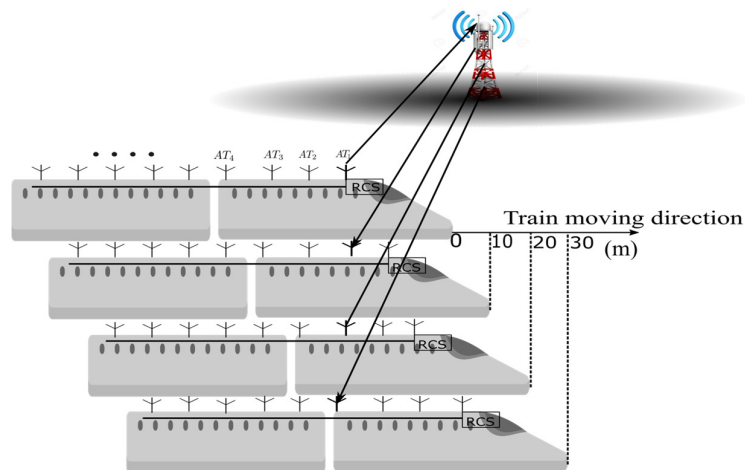


Figure 2.9: RADIATE architecture

for every 10m so that virtually for the macro cells BS the train antenna does not move [34]. Assuming a train moves 10m every RTT ($70 - 140ms$) when the velocity of the train is 100m, the distance between AT_1 and AT_2 is 10m. Therefore, if there is control

station tracking the movement of the train, after sending a SYN request signal to BS from AT_1 , the ACK comes to the train at 10m from AT_1 , where in RADIATE, AT_2 exists. Therefore, for the BS no virtual movement happened. Thus, the Doppler shift can be virtually reduced. However, with increasing speed of the train and reducing RTT for 5G network eventually, the train needs control station to store and estimate the position of the received signal at every $1ms$ interval introducing additional processing delay in communication. The overhead of processing at every sub-millisecond RTT for a dense RADIATE deployment, will introduce a very complex architecture.

Chapter 3. 5G PHYSICAL LAYER CONDITIONS

The fifth-generation communication technologies are going to be evolved from the LTE evolution to provide a wide-array of services to the end users. The interesting trend towards increasing spectral efficiency, throughput with optimized power consumption and latency in channels provide an overview of aggressive nature of future networks. According to IMT 2020, the roadmaps drawn covers from mobility aspects up to 500 km/h to achievable and average throughput of 20Gbps and 100Mbps, low latency and reliable communication. A very generic overview suggests that requirement should be met within 2020 [35]. Figure 3.1 suggests the overview proposed by IMT-A

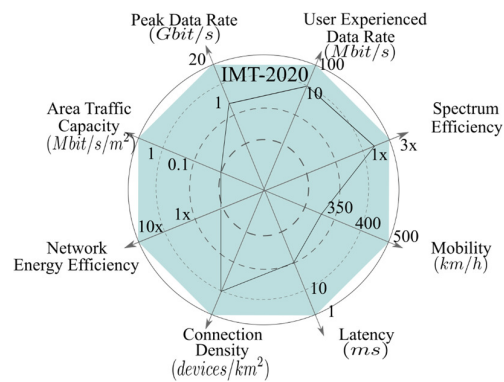


Figure 3.1: IMT-A (2020) goals

[20, 35]. Due to increasing demand of internet, rich multimedia and accessibility of devices to more people, a deluge of data in wireless network may happen. Most of the researchers suggest that in urban or suburban scenarios, ultra-densification, mmWave and MIMO can be some of the key technologies to discuss [36]. However, high-speed train mobility being our prime focus, in this chapter we broadened the scope to different physical layer considerations namely, mmWave, massive MIMO, beamforming and waveforms. The influence of mobility and major research organization involved in 5G project have been also discussed to give a summary of 5G.

3.1 5G in Mobility

The mobility requirements in 5G is mapped by the IMT-A and that it has to support a mobility of 500 km/hr. However, the modes to increase the capacity with different key technologies involved in 5G, integrates additional challenges with mobility. Majority of the technologies involve making the next generation communication an ultra-dense network from the device side perspectives. Figure 3.2

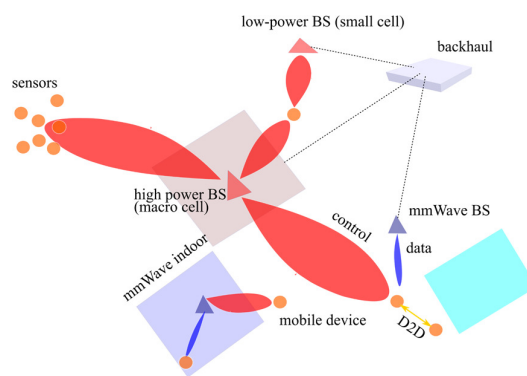


Figure 3.2: 5G device centric architecture

shows a detailed architecture overview [19]. The scope encompasses a device centric view of next generation wireless systems, where indoor and outdoor communication systems work together with machine type communication. The device centric architecture eventually depends on several different architecture considerations, which starts with making cells smaller, reusing frequency and continues with using heterogeneous networks for mobility, reducing round trip delay, cost and energy. One of the ways to support mobility is to use heterogenous network and utilize their consolidate gain, which eventually supports the claims of network densification. Doppler spread being one of the major cause of channel fluctuation in a high-speed mobile network, RTT of 5G being 1ms provides a major opportunity to reduce the

Doppler spread. However, this leads to a tradeoff between sub-frame size consideration and achievable throughput.

In a typical HST scenario, the base stations are deployed linearly. Typically, providing a reliable network architecture of HST depends on minimizing communication channel irregularities and less number of handovers. The specific challenges related to mobility in 5G networks are mentioned in [16] as,

- a) The highly mobile users will be serviced by microwave and lower frequency BSs instead of the mmWave BS comprising of their data rate.
- b) Modelling and analyzing mobility on network performance are hard.
- c) Define logical or virtual cells to remove handoff totally in physical cells for constantly roaming users can be challenging.
- d) A method of opportunistic handover should be attained and the concept of handover in layer 3 should be changed.
- e) Handoffs at mmWave frequencies are challenging since the need of alignment in transmit and receive beams.

The solution of these challenges can be through using multiple coordinated mmWave BS. In a linear coverage scenario BSs are deployed linearly, but in an urban scenario the BSs can be densely deployed to achieve a densification gain $\rho > 0$ to increase data rate and can be used with DAS or CoMP. The challenges in key technologies are mentioned in next sections separately. We propose next with an optimized number of small cell BSs to achieve a densification gain for HST scenario with the challenges involved in this specific environment.

3.1.1 5G in High-speed Train

It has been previously discussed that HST environment creates additional challenges for mobile communication. The focus of this research is to observe if moving to fifth generation communication systems solves some of the problem or brings some more issues without solving previous ones. Previous sections discussed mobility related challenges in fifth generation communication network and how different researchers attempting to address the issues. Our research primarily focused on 5G and HST and how to solve specific issues related to HST environment.

3.1.1.1 Channel Variations and Estimation

Channel variations in HST environments are affected by Doppler effects. Fast fading variation caused by Doppler Spread causes difficulty in tracking, estimating and predicting fast-time varying channel conditions. Table 3.1 shows the ICI mitigation techniques from [16]. The requirement for ICI mitigation falls into the category of efficient channel estimation within lower time complexity.

Table 3.1: Comparison of ICI mitigation techniques [16]

ICI mitigation methods	Operator	Performance
Direct ICI mitigation method	Joint estimation of CSI and CFO	Low Complexity, degrade quickly with Doppler shift (not suitable for mmWave)
Iterative ICI mitigation	Parallel interference cancellation	Effective, high complexity, error propagation for high mobility, not suitable for delay-intolerant services
Position based ICI mitigation	Utilize position information	Medium complexity and robust against Doppler shift, can be used with UCDA

Due to Doppler shift, the complexity of receiver increases due to its tracking capability. Time and frequency spread in communication channel further degrades communication links. In OFDM, fast time-varying channels change single to multiple symbols over time during transmission, resulting in a requirement of large frequency

and time resources to accurately estimate Channel State Information (CSI) [16]. This however leads to additional delay in RTT and not favorable towards 5G architecture.

Alongside CSI, ICI in OFDM systems severely degrades link performance due to carrier frequency offsets affecting orthogonality within subcarriers. Therefore, estimating CSI and mitigating ICI remain as challenges in HST 5G networks. Considering, control stations to handle both ICI mitigation and CSI estimation would add a processing delay in RTT from both transmitter and receiver side. Therefore, the unwanted delay in 5G architecture due to complex receiver side processing, compromises the IMT-2020 promises of sub-milliseconds aggregated delay in communication.

3.1.1.2 Signal Processing

As previously discussed, ICI, self-interference, inter-cell interference and other complicated interference degrade network and link performance in HST communication. Only advanced modulation, coding, precoding, newer waveforms, and diversity techniques will lead to a reliable channel performance when realizing 5G.

3.1.1.3 Large Scale Fading in mmWave

Large-scale fading has been heavily researched and discussed field in HST environment for microwave frequencies. The major research challenge to find path loss component and log-normal shadowing in the environment. However, in previous studies, path loss has been individually considered. In mmWave frequencies, the additional environmental losses such as rain loss, fog loss, etc. become significant attenuation factor. A frequency in range between 30-300 GHz and some available spectrum in 20-30 GHz are usable mmWave Frequencies. The wavelengths in this region can be from 1-10mm. Considering, fading losses in mmWave frequency for

high-speed would be a better bet for accurate channel estimation. Therefore, mmWave related path loss, rain and fog loss have been discussed in following.

- a) **Path loss:** The antenna sizes shrink and effective aperture scale with $\frac{\lambda^2}{4\pi}$, along with the higher frequencies [36]. The Free Space Path Loss (FSPL) grows with carrier frequency f_c^2 . Therefore, increasing frequency from 3-30 GHz will increase the path loss up to 20dB. Figure 3.3 shows the FSPL for 10-100 GHz frequency for 100m-10km distances, which depicts the

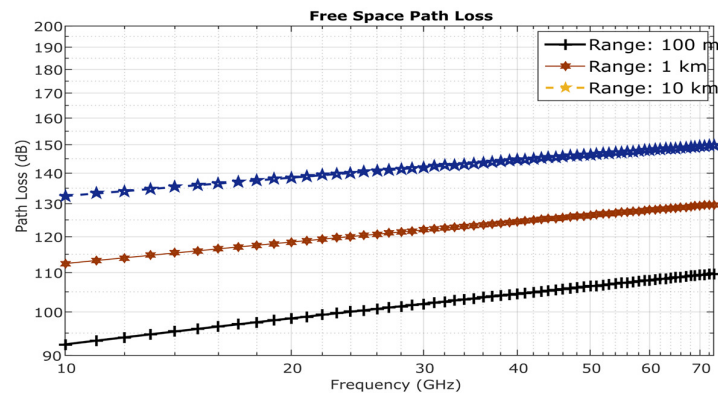


Figure 3.3: Free Space Path Loss (mmWave)

increasing path loss in mmWave frequencies. However, keeping the antenna aperture constant with increasing frequency, FSPL also remains constant. If the aperture size in both transmitter and receiver remain constant, the path loss *decrease* with a scale of f_c^2 [36]. However, our research primary focused on two different path loss models, which are Close-In Reference (CIR) distance and Alpha-Beta-Gamma (ABG) path loss models [37, 38]. The equation for BG path loss is given by (3.1),

$$\begin{aligned}
PL^{ABG}(f, d)[dB] & \\
&= 10\alpha \log_{10} \left(\frac{d}{1m} \right) + \beta + 10\gamma \log_{10} \left(\frac{f}{1 \text{ GHz}} \right) \quad (3.1) \\
&+ \chi_{\sigma}^{ABG}
\end{aligned}$$

Where, $PL^{ABG}(f, d)$ denotes path loss in dB over frequency $f = f_c$ and train antenna to 5G base station distance d , α and γ are coefficients dependent on d and f , χ_{σ}^{ABG} is the standard deviation for large scale fluctuations. On the other hand, the path loss based on CI model is given by (3.2),

$$PL^{CI}(f, d)[dB] = FSPL(f, 1, m)[dB] + 10n \log_{10}(d) + \chi_{\sigma}^{CI} \quad (3.2)$$

Where, n denotes the single model parameter, the Path Loss exponent (PLE), with a reference distance of 1 m. The FSPL at distance d ,

$$FSPL(f, 1, m)[dB] = 20 \log_{10} \left(\frac{4\pi f}{c} \right) \quad (3.3)$$

Where, c is the speed of light. Figure 3.4 shows the path loss of Urban Micro Street Canyon scenario for 28 and 73 GHz. The figure shows that a significant path loss is inevitable in even regular environments. The large path loss does not only force to increase the power of the transmission but also increase the receiver sensitivity. Considering a LTE receiver having

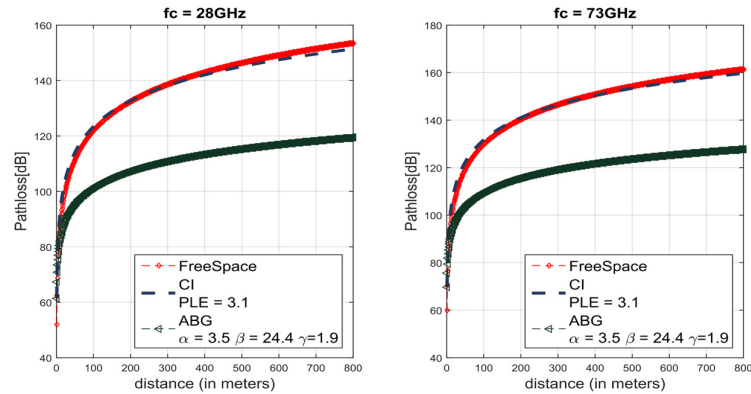


Figure 3.4: Street Canyon UMA pathloss model for $f_c=28$ and 73 GHz

receive sensitivity of -73 dB, in a HSR scenario it is required to increase the signal strength with femto cells or Mobile Relays (MR) [39].

Maintaining the electrical size of antennas is highly desirable with increasing frequency. Therefore, utilizing large antenna arrays with more number of antennas in a physical region to aggregate the aperture size, the path loss can be constrained [36]. In an HST environment, physical orientation of devices does not change considering minimal indoor movement, femto cell access points and almost linear movement of trains. However, Doppler shifts in mmWave creates difficulty in co-phasing multiple array antennas to steer them properly.

Additional to path loss, atmospheric losses are also significant causes of degrading channel performance.

b) **Rain and Fog loss:** In mmWave frequencies atmospheric losses are significant [36]. The absorption losses due to rain has been shown in Figure 3.5. The figures shows that a significant loss may prove additional degradation in signal and in mmWave frequencies rain loss can become more than 10dB/km. Considering the air absorption mmWave frequencies there are some frequencies where it may seem inconsequential. Selecting those frequencies for urban and rural HST environments may become highly

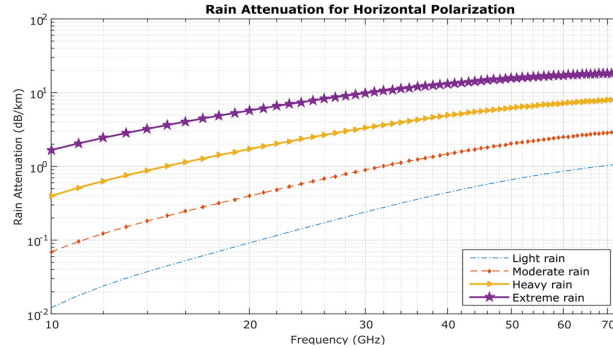


Figure 3.5: Rainloss for mmWave frequencies

effective for physical deployments [36-39]. Our research concluded 28 & 73 GHz to be the most suitable for current mmWave deployments due to their comparably lower air absorption losses. Whereas, a 60 GHz frequency used in 802.11ad can be affected by a 15 dB/km oxygen absorption [36]. The frequency is mostly proposed in different RoF architectures for cell on edge deployments.

According to different researchers, propagation losses for mmWave frequencies cannot be an insurmountable problem [36]. It requires a large number of array antenna to properly steer it and for coherent recollection. The mmWave antennas transmit

highly directional and narrow beams. Due to narrow beams, interference is occurred often, but, can adopt an on/off behavior.

In a high-speed environment transmitting and receiving antennas have to employ to scan a multitude of positions to find the narrow beam in transmission. This adds in additional challenges in rapidly time varying environment. Therefore, we move into exploring key technologies to address certain challenges in 5G.

3.2 Key Technologies in 5G

The ways to achieve an improvement in network throughput can be simply calculated by below formula,

$$\underbrace{\text{Throughput}}_{\text{bit/s/km}^2} = \underbrace{\text{Available spectrum}}_{\text{Hz}} \cdot \underbrace{\text{Cell density}}_{\text{cell/km}^2} \cdot \underbrace{\text{Spectral efficiency}}_{\frac{\text{bit}}{\text{s}}/\text{Hz}/\text{Cell}}$$

The ways to get more spectrum can be by mmWave frequency bands and with ultra-dense deployments we can increase cell density. But, higher spectral efficiency can be achieved by Massive MIMO.

3.2.1 Densification

Densification in HST environment is completely different than regular hexagonal environment except in urban deployments. In trivial HST environment, the small cell BS densification can be considered alongside UCDA, and increase the number of mmWave BS under single macro cell to increase densification gain ρ . To achieve a data rate of C_1 with small cell BS, density can be of $\lambda_1 \text{ cells}/eNB$. Considering a higher BS density of $\lambda_2 \text{ cells}/eNB$, with corresponding rate of C_2 , then densification gain is given by,

$$\rho = \frac{C_2 \lambda_1}{C_1 \lambda_2} \quad (3.4)$$

Increasing data rate through cell densification is straightforward. Having twice the network density means increasing throughput twice and $\rho = 1$.

3.2.2 Massive MIMO

For HST environment, massive Multiple Input Multiple Output (MIMO) are being used to achieve higher capacity and reliability. MIMO comprises of spatial dimension of the communication arising with multiplicity of the antennas available in BS and UEs [36]. In Single User MIMO (SU-MIMO), the dimensions are limited by the number of antennas used in a limited space. However, multi-user MIMO (MU-MIMO) can avoid the constraints of SU-MIMO by concurrently transmitting to multiple users, or train antennas. The CoMP scheme previously discussed can further remove the bottleneck by achieving a joint transmission and receiving scheme with multiple BS. Therefore, it can turn some of the inter-cell interference into effective signal.

The scope of realizing massive MIMO in 5G and high-speed mobility is to use many low power amplifiers fed massive number of antennas. Therefore, there is a required power gain/interference reduction and parallelization tradeoff. In our research, we mostly focus mmWave and small cell BSs. The small cell BSs are the least suitable for massive MIMO deployment. The reasons are mostly due to form factors and decreasing number of users covered by small cells. However, mmWave cells may require a lot more antennas for proper beam-steering and beamforming [36]. The wavelength being smaller in mmWave a large number of antennas can be fit into the transmitter BS or UE, which is already discussed. The devices can provide

beamforming power gain and MIMO opportunities due to large number of antennas and conformal array designs [36].

3.2.2.1 Stationarity and Nonstationarity

Massive MIMO behavior in stationary and non-stationary channel is different, where stationary channels are based on the Tx power gain. However, time variant property of mobility adds more challenges in MIMO communication. Due to future ultra-dense deployment, conventional LTE will face increased number of handovers, in high mobility the handovers will be done within short period of times, resulting in handover failures. Due to a 5G requirement, RTT in air interface has to be $\leq 1ms$ including Hybrid Automatic Repeat Request (HARQ). A subframe length or Time Transmission Interval (TTI) of $200\mu s$ is required to guarantee the RTT. Therefore, it is required to have both narrowband and wideband channel access [40]. Narrowband channel access can be maintained to track users in high-speed environment even without data transmission and wideband channel can be used to provide CSI for efficient MU-MIMO resource allocation.

In [41], non-stationary wideband MIMO channel model for HST has been proposed. The small-scale fading such as Angle of Arrival (AoA) and Angle of Departure (AoD) have been considered in the model. The models assume finite and infinite number of scatterers, and the statistical parameters are also defined [41]. It is also extended for different scenario specific channel environments. The channel impulse response of the HST channel model between the p -th transmitter and q -th receiver can be expressed as from [41],

$$\begin{aligned}\tilde{h}_{pq}(t) &= \tilde{h}_{1,pq}(t) + \tilde{h}_{i,pq}(t) \\ &= \tilde{h}_{1,pq}^{LOS}(t) + \tilde{h}_{1,pq}^{SB}(t) + \sum_i h_{i,pq}(t)\end{aligned}\quad (3.5)$$

Where,

$$\tilde{h}_{1,pq}^{LOS}(t) = \sqrt{\frac{K_{pq}(t)}{K_{pq}(t) + 1}} e^{-j2\pi f_c \tau_{pq}(t)} e^{j2\pi f_{max} t \cos(\tilde{\phi}_{T_p}^{LOS}(t) - \gamma_R)} \quad (3.6)$$

$$\begin{aligned}\tilde{h}_{1,pq}^{SB}(t) &= \sqrt{\frac{\Omega_{1,pq}}{K_{pq}(t) + 1}} \sum_{n_1=1}^{N_1} \frac{1}{\sqrt{N_1}} e^{j(\psi_{n_1} - 2\pi f_c \tau_{pq,n_1}(t))} \\ &\quad \times e^{j2\pi f_{max} t \cos(\tilde{\phi}_R^n(t) - \gamma_R)}\end{aligned}\quad (3.7)$$

$$\begin{aligned}\tilde{h}_{i,pq}(t) &= \sqrt{\Omega_{i,pq}} \sum_{n_1=1}^{N_i} \frac{1}{\sqrt{N_i}} e^{j(\psi_{n_1} - 2\pi f_c \tau_{pq,n_1}(t))} \\ &\quad \times e^{j2\pi f_{max} t \cos(\tilde{\phi}_R^{n_i}(t) - \gamma_R)}, \quad 1 < i \leq I\end{aligned}\quad (3.8)$$

All the parameters such as, $K_{pq}(t)$, $\tau_{pq}(t)$, $\tilde{\phi}_{T_p}^{LOS}(t)$, $\tau_{pq,n_i}(t)$, $\tilde{\phi}_R^{n_i}(t)$ are time-variant in nature. The $\tau_{pq}(t)$ depends on the distance between transmitter and receiver, whereas, $\tau_{pq,n_i}(t)$ can be obtained from a relationship between transmitter and effective scatterer distance, and, receiver and effective scatterer distance. ψ_{n_i} is the uniformly distributed initial angular values, where γ_R denotes the angular motion.

3.2.3 Beamforming

The next generation wireless system depends on narrow and focused beams, which will be complex to design. Using mmWave frequency makes the beamform narrower and highly directional, which makes the beams very sensitive to misalignment

and interference. Overall using massive MIMO may make the communication interference limited, but with mmWave beamforming interference may get de-emphasized and channel becomes noise limited [36, 42].

The challenge in beamforming is in difficulty in establishing communication between train antenna and BSs. The short period in handoff and initial connection make it more challenging for seamless connection. Even to find each other, they have to search a lot of angular positions. Even the complexity rises with effective beamformer designs, which is becoming more analog than digital to avoid massive power consumption [43].

3.2.4 Waveforms

With change in generations, the basic change in PHY design has been opted in waveform designing. In 1G, FDMA has been widely used, while in 2G FDMA and TDMA both have been used, but majorly known as, ‘TDMA’ for time-multiplexing. However, in 3G the monotony of TDMA and FDMA ended with CDMA, but with limitations in high-speed data [36]. Due to increasing demand of channel bandwidth, OFDM came into picture with scheduled FDMA/TDMA. Therefore, in 5G newer waveforms are bound to advance the scope of next generation communication to support future needs.

Chapter 4. WAVEFORMS IN 5G

The waveforms are one of the aspects where PHY and MAC layers of next generation wireless system may provide a better reliability scheme in high-speed mobility. For an ideal waveform scheme for HST environment may provide support for [20],

- a) High spectral efficiency with higher throughput.
- b) Low peak-to-average power ratio (PAPR) allowing efficient power amplifier design for better receiver sensitivity.
- c) To support mobility, the waveform should be capable to be robust against Doppler shift
- d) Support asynchronous transmission and reception for a UCDA.
- e) Excellent pairing with MIMO allowing spatial interference from multi-antenna

In Gabor's "Theory of Communication", a multi carrier system such as OFDM, should follow the following design considerations [44],

- a) The subcarriers are mutually orthogonal in both time and frequency domain to keep receiver complexity and ICI low
- b) Transmission function provides localization capability in both time and frequency to obtain immunity from multipath propagation based delay spread and ICI. For low latency transmission, time based localization is required.
- c) Maximal spectral efficiency is considered as, $se = (T\Delta f)^{-1}$, with se being the spectral efficiency in $bits/s/Hz$.

However, the challenge is fulfilling three constraints altogether. It should be noted only two out of three can be obtained at the same time which in turn affects design choices of 5G waveform.

4.1 Waveform Candidates

The goal of newer waveforms is to find the limitation of OFDM and go beyond OFDM. We discuss three new waveforms in the next sections due to certain limitation of OFDM. The limitation extends to, high PAPR in OFDM, due to envelope samples being Gaussian through the summation of uncorrelated inputs in IFFT [20]. High PAPR sets constraints towards building power amplifier and the linearity of the transmitted signal. Spectral efficiency of OFDM signals also are restricted. The Cyclic Prefix (CP) used in addressing ICI also reduces spectral efficiency. The major concern regarding OFDM is though power amplifier design. The nature of radio being software defined and virtually controlled network, FFT block size, subcarrier spacing and the CP length can change with channel condition for a better performance, depending on channel conditions. For abundance of bandwidth, the subcarrier spacing can grow with FFT size and CP being optimum for enhanced spectral efficiency. However, HST environment restrains the OFDM conditions to be narrower subcarriers, longer FFT blocks and a longer CP. Attaining a sub-millisecond delay in HST environment made the researchers look for other waveforms. The major waveform candidate waveforms are based on non-orthogonality and proposed as 5G Non-Orthogonal waveforms or ‘5GNOW’.

4.1.1 FBMC

Filter-Bank Multi-Carrier (FBMC) applies a filtering method at subcarrier level and filtering blocks both at transmitter and receiver [20, 45, 46]. The different implementation of FBMC involves: - Staggered MultiTone (SMT), Cosine Modulate MultiTone (CMT) and Filtered MultiTone (FMT). However, major focus for waveform design is on SMT, even in HST environment. For different simulations SMT is being used extensively. Figure 4.1 shows transmitter blocks. In this block, FIR prototype filter is being used based on Root Raised Cosine (RRC) with a roll off factor 0.1 for N polyphase filter A_k of length K . K determines the overlapping factor for filter

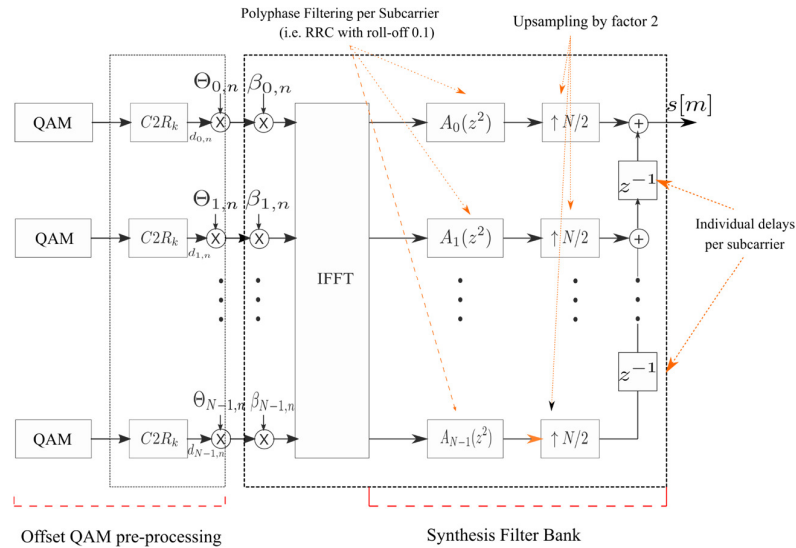


Figure 4.1: FBMC transmitter blocks

characterization. It has been decided to use 4 as a standard for FBMC [20]. In the filter bank created by $\frac{k}{N}$, frequency shift impacts orthogonality with energy spread towards neighboring subcarriers. However, the orthogonality is maintained between even and odd subcarriers.

FBMC supports a very long propagation delays and arbitrarily high frequency offsets [47]. As, OFDM requires very high CP to support HST environment, FBMC can be

very efficient replacement in place of OFDM to increase spectral efficiency. FBMC uses Offset Quadrature Amplitude Modulation (OQAM) scheme to maintain orthogonality within real and imaginary domain. OQAM is achieved by shifting in-phase components half the symbol length compared to out of phase components. Interference is reduced at every second sub-carriers and OQAM rejects ICI, avoiding the received signal carrying the data [20, 47]. However, as previously mentioned, FBMC would accommodate more implementation complexity with larger FFT window size, etc. Figure 4.2 shows the FBMC waveform in comparison to OFDM in Power Spectral Density (PSD) with normalized frequency.

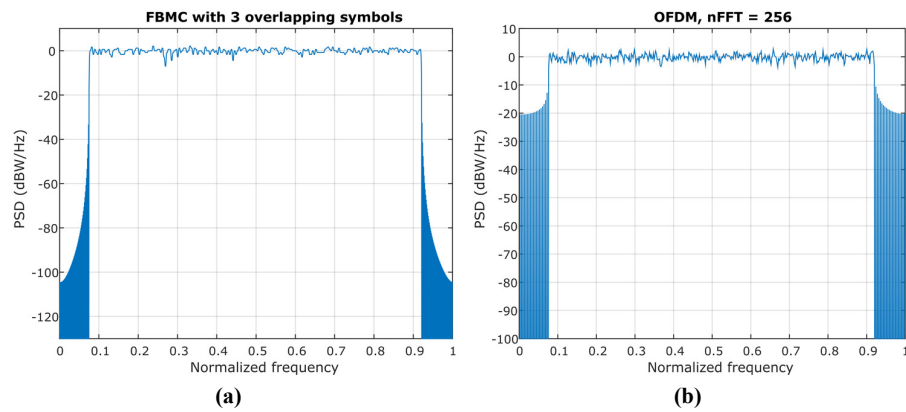


Figure 4.2: Waveform PSD comparison between FBMC and OFDM

4.1.1.1 Advantages

- a) Asynchronous transmission can be done, therefore, constrained synchronization such as in LTE is not needed. Architectures like UCDA where lack of synchronization may cause signal degradation, FBMC would be a significant attribute to the architecture.
- b) Applications like spectrum sharing for fragmented spectrum.
- c) FBMC is very much suitable for high-speed environment and should be exploited thoroughly in HST environment.

However, FBMC may sound advantageous for HST environment and UCDA, there are some disadvantages involved.

4.1.1.2 Disadvantages

- a) The pilot being scattered make the waveform more complex
- b) Space time coding, which are highly recommended for HST communication is complex.
- c) Uplink and frequency selective beamformings require 1 carrier guards each.
- d) Short bursts are disadvantageous for long filter trails.

The argument presented by Schaich in [47] is, using LTE with FBMC, during multiple user sharing the same channel, user transmission may interfere with each other at the frequency edge. This degrades the orthogonality in OQAM. Therefore, the only solution is using multi-user guards, which can be introduced in HST environment with femto cells and DAS schemes.

4.1.2 UFMC

UFMC or Universal Filter Multi-Carrier groups sub carrier into filtered sub-bands [20, 47]. To prevent aliasing, the number of carriers per sub-band are standardized. UFMC also provides flexible utilization of the available spectrum utilizing filtering operation for entire frequency band. Figure 4.3 Shows the transceiver design of UFMC [47, 48].

The implementation complexity of UFMC can be compared to FBMC due to FFT window size. UFMC also includes optional usage of guard intervals as CP. As there is no time overlap between subsequent symbols, the symbol duration is $N + L - 1$, where

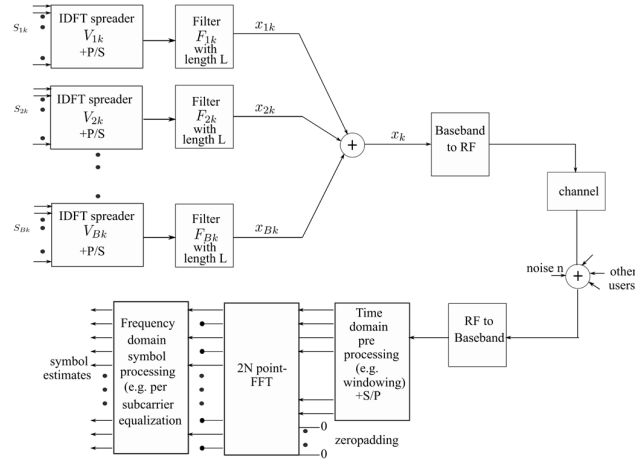


Figure 4.3: UFMC transceiver design

N being the FFT size and L being the filter length. UFMC supports short bursts traffic for low latency transmission. The block wise filtering employs additional filtering to account for OFDM CP. Below, UFMC is considered as generalized UFMC and FMT to provide brief idea how the transmission vector can be generated.

The time-domain transmit vector for a multi-carrier symbol for user k , being superimposed sub-band filtered components, is shown as [47],

$$X_k = \sum_{i=1}^B F_{ik} V_{ik} S_{ik} \quad (4.1)$$

For each of B subbands, complex QAM symbols get converted to time domain by IDFT matrix by V_i . F is a Toeplitz matrix composed of filter impulse response to perform linear convolution. From the equation, it can be easily noted that there is no time overlap between subsequent UFMC symbols previously discussed. Figure 4.4 shows the transceiver chain output,

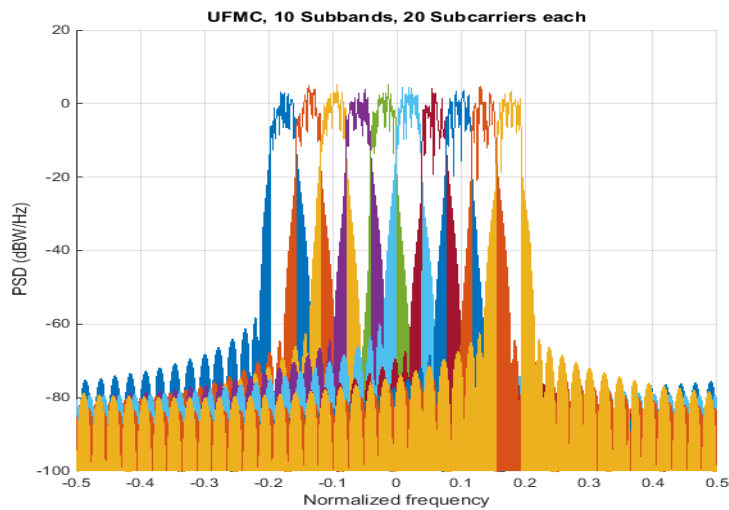


Figure 4.4: UPMC waveform with 10 subbands

4.1.2.1 Advantages

- a) High spectral efficiency similar to FBMC
- b) Less overhead than FBMC
- c) Supports short burst transmissions
- d) Support for low-latency channels

4.1.2.2 Disadvantages

- a) UPMC can be rather be useful for control plane or delay-intolerant traffic where reliability and low-latency are the main requirements. High data rate cannot be always supported in UPMC.
- b) High delay spread enforces it to use multi-tap equalizers
- c) Similar to FBMC, larger FFT size makes the implementation harder
- d) There will be significant interference from overlapping sub-bands (not subcarriers)

UPMC is targeted towards machine-to-machine communication, with low latency and low bandwidth operation. For HST environment, UPMC has clear

advantage to maintain sensor network communication in in-train network reliably.

4.1.3 GFDM

Generalized Frequency Division Multiplexing (GFDM) uses filter bank multi-carrier techniques to spread the spectrum towards each user space as multiple spectral segments. Generally, GFDM being derived from FBMC it can be used for spectrum sharing and deployed in HST environment for train control service channels as,

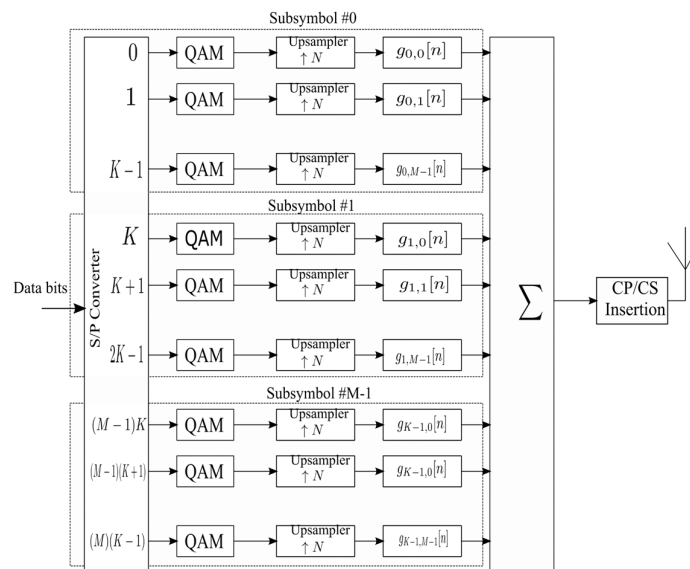


Figure 4.5: GFDM transmitter

- Figure 4.5/4.6.a provides the transceiver design.
- CP is still introduced to avoid ICI but can be introduced after multiplexing or before filtering [20, 49].
- Each subcarrier having different bandwidth, prioritized access control and spectrum sharing can be employed. Different train and passenger services can be launched with different priority with optimized access control through the subcarriers.

- d) The filtering is done by circular convolution with standard number of symbols, which is named as tail biting. That results in segmentation in time domain [49].

In Figure 4.5, $g_{k,m[n]}$ is impulse response of a filter with N samples, where k , m and n are subcarrier, subsymbol and time indices [20, 49]. In GFDM also, data is transmitted in MAC layer block wise. However, each block has CP and several sub-symbols. This decreases spectral efficiency. For delay tolerant services all the sub-symbols can carry user data where in delay intolerant services only certain sub-symbols carry data. However, GFDM receivers are complex due to additional equalization and interference cancellation. Figure 4.6.a shows the receiver design of GFDM, where, the waveform in comparison with OFDM is shown in Figure 4.6.b.

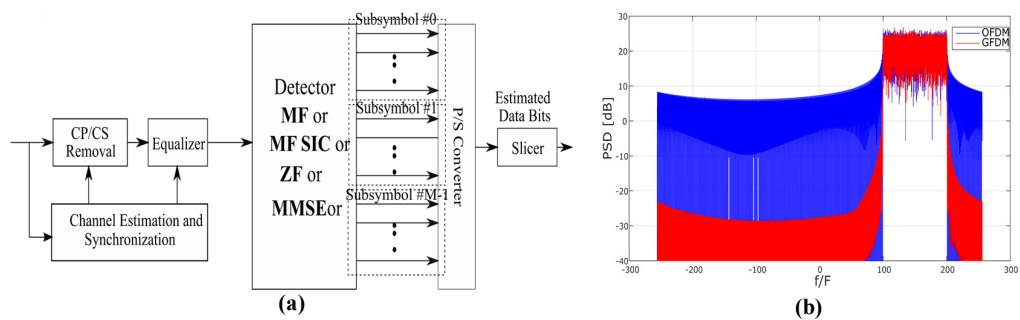


Figure 4.6: GFDM receiver (a) and waveform (b)

4.1.3.1 Advantages

- Comparatively lower PAPR
- Very low out of band leakage due to adaptable Tx-filtering
- Multi user scheduling can be possible in time and frequency domain
- White space aggregation possible in even heavily fragmented spectrum region.

4.1.3.2 Disadvantages

- a) Very complex receiver design
- b) In a HST environment, to remove ICI, matched filter must be used and also MIMO design is complicated through using OQAM.
- c) Symbol Time Offset (STO) and Carrier Frequency Offset (CFO) are required
- d) A complex higher order filtering and tail biting are required to suppress ICI, which make it hard to implement in HST environment.

Following the advantages and disadvantages, GFDM has considerable advantages over UFMC where, it performs as close to FBMC. Therefore, GFDM is highly suitable for cognitive radio rather than high-speed mobility environment with low latency requirement. However, GFDM can be suitable candidate for PTC and rail-CR regarding its performance in fragmented spectrum region. However, the operation should be in a reasonable mobility.

4.2 Selecting Waveform Candidate for HST Environment

As it is previously discussed, what are the requirements to become 5G waveform candidates, HST environments integrates some more challenging constraints. To adapt to these challenges, like relaxing synchronization requirements or controlling out of band emissions, the newer waveforms employ filters [45-51]. In a HST environment, however, FBMC has been largely considered over OFDM and other waveforms due to [12, 16],

- a) Simultaneous connections can be made between different trains, users and railcars with allocating the resources in scarce spectrum available. It can be possible because of high bandwidth efficiency in FBMC.

- b) For co-existence issues with GSM-R and new broadband systems, FBMC provide an efficient co-channel interference mitigation.
- c) Since FBMC uses frequency localized subcarriers, it avoids multiple access interference. The waveform being asynchronous a ‘*close-to-perfect*’ carrier synchronization is not required in highly mobile communication channels.
- d) FBMC performs better than OFDM in doubly-dispersive channels which is very common in HST environments. However, OFDM being defined as rectangular window in time domain, it seems unbounded in frequency domain. In HST communication, delay spread affecting channel response in both time and frequency domain, only FBMC can operate and perform better in doubly selective channels due to the filters that can offer better performance in both time and frequency domain.

4.3 A Comparative Result with FBMC

It is proposed in [12], when the normalized Doppler spread of the channel is given by, $D_n = f_d T$, f_d being the maximum Doppler frequency and T denoting the FBMC symbol period. T in SMT is $T_{SMT} = \frac{T_s N_c}{2}$. The parameter T can be adjusted by time interpolation factor I , complimenting FBMC symbol period $T^{(I)} = IT$. Therefore, the bandwidth becomes I times narrower with reduced subcarrier spacing. Therefore, the normalized Doppler spread will affect time-interpolated FBMC as where the train velocity is v ,

$$D_n^{(I)} = f_d T^{(I)} = f_d IT = \frac{IT f_c v}{c} = \frac{T f_c}{c} v^{(I)} \quad (4.2)$$

Where, $v^{(I)} = Iv$ is the emulated speed of an actual measurement speed v . The evaluation setup for the consideration is shown in Figure 4.7, where, P_T

and σ_w^2 denote the transmitted power and noise variance for the high-speed mobility emulation process.

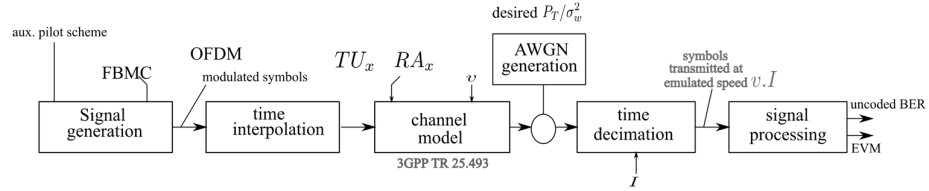


Figure 4.7: Emulation setup for High-speed mobility

4.4 NYU simulator

New York University (NYU) has been involved in channel sounding of mmWave communication systems for a while. The simulator can be used to show different physical layer considerations with small scale fading parameters

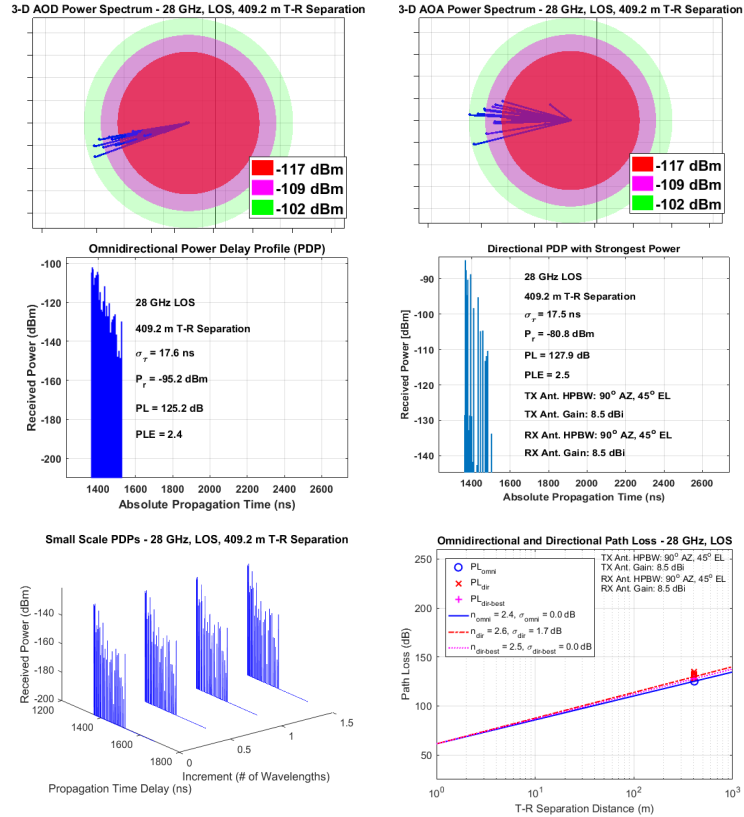


Figure 4.8: NYU Wireless Simulation Results

[52]. Due to consideration of practical measurements from mmWave channel sounding by NYU wireless lab, it makes the simulator a better stage for further linear high mobility movement based channel modelling. The simulator does not assess a high-speed train scenario. However, based on the measurements, it can be possible to move from stationary wideband to nonsationary wideband MIMO channel simulation. To provide an overview of HST and mmWave frequency simulation, we considered Tx/Rx azimuth and elevation at 90^0 and 45^0 , due to BS antenna and train antenna being at same height. Rural Macro (RMa) LOS environment with $f_c = 28$ GHz and bandwidth being 800 MHz, for 4 antenna Tx/Rx scenario, the simulation results are presented below with Figure 4.8.

Chapter 5. USER AND CONTROL (PLANE) DECOUPLED ARCHITECTURE (UCDA)

The chapter discusses about the physical decoupling of user and control plane with different frequencies and utilizing the decoupled architecture in HST environment to ensure reliability and provide high capacity to passengers.

5.1 The UCD Architecture

As we previously discussed, LTE-R is one of the potential replacement of GSM-R in HST communication. However, From Table 2.1, it can be seen that due to guaranteed low capacity, in HST environment LTE-R does not provide an integrated solution. Moreover, LTE-R is primarily targeted towards railway operation, signaling, control communication. Therefore, ideally including passenger data degrades LTE-R performances and overall reliability.

For a long time, HST have become a lucrative travel option to the passengers. Due to increasing number passengers in HST lines over continents, the demand of in-train Wi-Fi as a basic amenity is also increasing. Depending upon only one radio access method to provide seamless connection to passengers, could never be possible. For many years, academia and industries introduced different solutions for high-speed, namely: railway environment targeting multiple radio access methods, heterogenous network, enhancing NLOS communication channel performance through femto cells, RoF and leaky coaxial cables, distributed antenna systems on track etc. alongside backhaul wireless communication. However, most of the research targeting heterogeneity, do not especially focus on reliability of basic train performance or forward compatibility towards adapting newer radio access methods without

disrupting the regular HST operation [1]. In most of the cases, the technologies are used together to support more capacity for passengers. Nevertheless, the lack of backhaul and very scarce dedicated channel bandwidth, it is not possible to look forward towards future and provide the passengers the same number of services that they enjoy in non-mobile wireless or wired connected environment.

The concept of user and control plane decoupling architecture first came from [30] to enhance the performance of LTE-B. The architecture mainly exploits a heterogeneous network with macro and small cells. It has been discussed increasing several small cells, i.e., micro, femto and pico cells increase the area spectral efficiency and capacity to an overwhelming 1000-fold [29]. Small cells also extend the coverage, optimize power consumption, and increase spectral efficiency, alongside control the receiver side power consumption.

Kishiyama *et al.* in [29, 53] proposed that, there is a large signaling overhead considering the huge number of devices involved in simultaneous communication. In traditional heterogeneous architecture, the small cells are involved in extending the coverage. However, including more number of small cells increase cellular interference and signaling overhead due the number of cells involved and due to abundant cells and mobility involved. A significant number of handovers due to mobility and connection for short period of time also degrade communication performance. The data and control plane decoupling encompass seamless connection of end-users through the control channel and only raw data can be transmitted through the small cells. This provides a seamless connection even in high mobility, because of control channel being constantly connected. The UCDA can be however compared with Software Defined Networks

(SDN). In SDN, the control channel is responsible for centralized routing. Table 5.1 compares two architecture in brief.

Table 5.1: Comparison between SDN and UCDA

Comparison topic	SDN	UCDA
Scope	Core or backhaul	RAN
Architecture elements	Routers	User plane
Core unit	Central controller nodes	Control planes
Advantages	Software defined upgradable, capacity, energy & cost saving	Robust in mobility and inter-cell interference, energy & cost saving
Challenges	Interim delay, single point of failure	Trivial definition of functionality and signaling decision within control plane, framing, front haul/backhaul flexibility, single point of failure

5.1.1 Phantom Cells

In UCDA, small cells can carry only data, without any signaling or controlling information. They are called '*phantom cells*'. The cells are completely dependent on macro cells to provide seamless end-user connection. Without macro cells, the small cells cannot work independently. However, due to the control plane being totally handled by the macro cells, the signaling overhead can be reduced to a large extent. Even with dense deployment of small cells, the signaling overhead can be controlled. Independent on the location or mobility the train can be connected to the macro cell seamlessly. The number of handovers also can be reduced with proper synchronization in place.

5.1.2 LTE Frames

The macro cells are lower frequency cells with low pathloss, thus contributing large coverage area. Whereas, small cells face larger path loss, but provide a larger bandwidth with smaller coverage area. The smaller cells can support increasing capacity demands. LTE is currently utilizing the bands below 2.5 GHz heavily and

provide 4G connection. 3GPP have been trying to utilize unlicensed spectrum and ISM bands for solving scarce bandwidth challenge, that does not guarantee fulfilling future capacity demands.

UCDA in LTE as we previously discussed proposed by [30, 54]. The concept extends by addressing existence of two planes User or U-plane and Control or C-plane served by the eNB. The System Architecture Evolution is responsible for the plane separation and there are two dedicated plane dependent modules involved. One is Service Gateway (SGW), which is responsible for dedicated user data transmission. And, second is, Mobility Management Entity (MME) which takes care of random access and handover signaling [30].

5.1.2.1 Frames and Channel Mapping

In a traditional LTE, the channel mapping includes a mapping from logical to transport and transport to physical channel mapping. A logical channel is also control channel due to control traffic carrying capabilities as [30], Paging Control Channel (PCCH), Common Control Channel for controlling and random access, Dedicated Control Channel (DCCH) for message configuration such as handover, Broadcast Channel Configuration (BCCH) to transmit messages to all users simultaneously, Multicast Channel for C-plane (MTCH) for Multimedia Broadcast Multicast Services (MBMS) downlink transmission. Multicast Control Channel (MCCH) for control channel transmission is required for MTCH and Dedicated Traffic Channel (DTCH) traffic channel for MTCH.

Among these channel mappings, BCCH, MCCH are responsible for control channel information or system level information, whereas, PCCH, CCCH, and DCCH carry specific user dedicated control channel data with paging, handover and random access data [30]. U-plane data is carried by DTCH and MTCH. Logically, both channel, U-plane and C-plane are mapped separately. But, as in Figure 5.1, they both converge

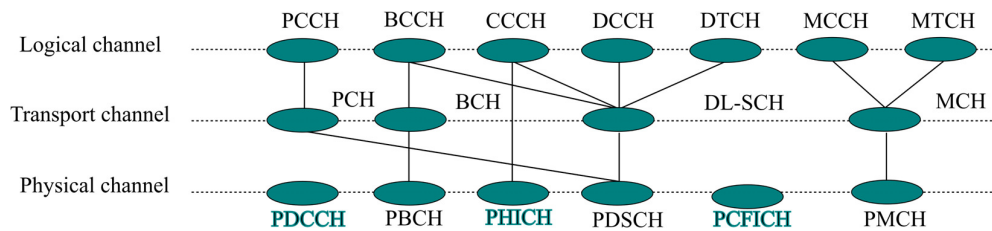


Figure 5.1: Conventional LTE frame structure

to a same transport and physical channel. These two planes can be physically decoupled and transmitted by two physical nodes as in Figure 5.2. Converged Physical Downlink

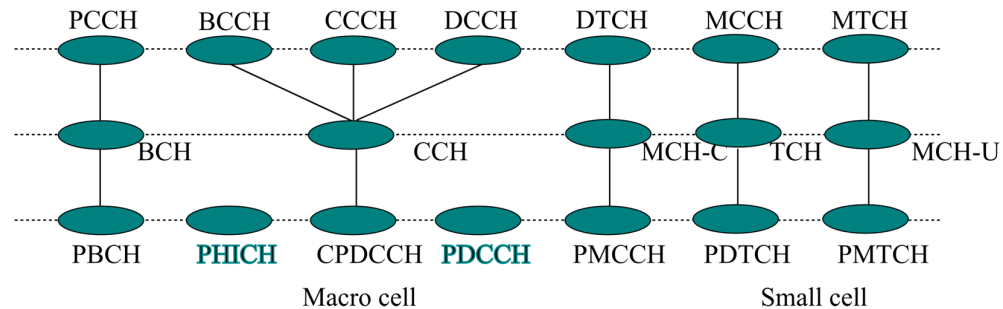


Figure 5.2: LTE proposed frame structure [30]

Control Channel can map PCCH, CCCH and DCCH being user dedicated control channel mapped to transport layer control channel (CCH) first. However, cell-dedicated control channels BCCH and MCCH, which carry different cell information, can be mapped separately to transport layer in two different channels, Broadcast Channel (BCH) and Multicast Channel for C-plane (MCH-C). After that, they can be mapped to physical channel as, Physical Broadcast Channel (PBCH) and Physical Multicast Control Channel (PMCCCH) [30]. C-plane and U-plane being moved to different frequencies, Physical Control Format Indicator Channel (PCFICH) is not needed for

differentiating control and shared channel boundaries. But, Physical Hybrid Automatic Repeat Indicator Channel (PHICH) and PDCCH are required to carry Hybrid Automatic Request (HARQ) feedback information and Downlink Control Information (DCI). Traffic channels, DTCH and MTCH are separately mapped to transport channels Traffic Channel (TCH) and Multicast Channel for U-plane (MCH-U) and afterwards to physical channels Physical Downlink Traffic Channel (PDTCH) and Physical Downlink Multicast Channel (PDMCH). Figure 5.2 provide the new channel mapping configuration.

5.1.2.2 Framing in PHY Layer

LTE has two physical layer frames, PDCCH and Physical Downlink Shared Channel (PDSCH) shown in Figure 5.2?. PDCCH is dedicated to carry controlling information for seamless connection between UE and eNB. Due to only logical separation of U-plane and C-plane in conventional LTE, the time and frequency resources are shared by both the planes in PDSCH. Due to physical separation in UCDA, [30] proposed a different framing architecture in LTE. In Figure 5.2, PDTCH is moved towards higher frequencies to support more capacity, and C-plane being reliability constrained, CPDCCH carries the C-plane information in lower frequencies.

5.1.3 UCDA and HST

In HST environment, user and control plane is defined and decoupled differently. As, lower frequency guarantees reliability, the control plane consisting train control information and passenger control plane are delegated towards lower frequency channels considered as control plane in HST-UCDA. Therefore, only bandwidth intensive user plane or traffic generated by the passenger services are moved into user or data plane which is serviced by higher frequency channels of LTE. However, these

division of traffic can be made through criticality and bandwidth requirement. If future train control data such as complete video monitoring is required and become bandwidth intensive, it can be moved to user plane of HST-UCDA. Therefore, the architecture remains very flexible towards connecting the in-train UE through Access Points (AP) or Mobile Relays (MR) to trackside eNBs. However, due to no control channel information, U-plane can be directly connected to SGW, without connecting it to MME. Figure 5.3 shows that simple control of small cells can be managed with X3 interface [30]. For stricter and time-constrained critical information transmission, C-plane of HST-UCDA, is connected to MME as well as, SGW.

5.2 Analysis of The Architecture

In HST-UCDA, the performance evaluation can be done through the handover performances and reliability evaluation. The authors in [30], propose CoMP to handle

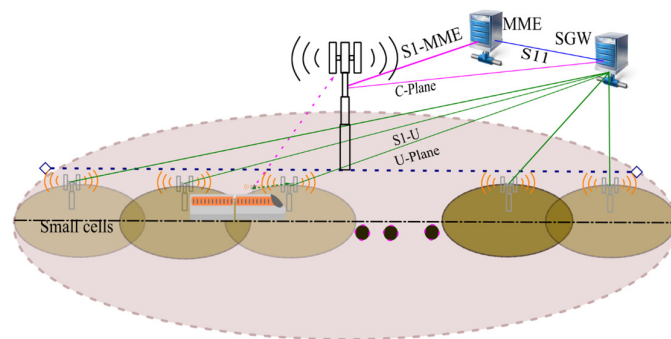


Figure 5.3: Complete Architecture of UCDA

small cell handovers and optimize the performance. Due to numerous small cells inside macro cells, several handovers can be possible, which in-turn degrades the architecture reliability. Using CoMP with small cells can enhance the performance and reliability to a large extent. However, it may increase the requirement for sophisticated synchronization.

5.2.1 Reliability of the Architecture

Determination of UCDA reliability is a special problem shown by [55]. Having two physically decoupled planes, it should be noted if the transmission of one plane affecting another. By design, C-plane is more reliable due to lower frequency channels than U-plane. However, the architecture reliability is not defined only through U or-plane individually. The reliability measurement should ensure both the plane contributions are captured.

5.2.1.1 Outage Probability

Outage probability has been a measure for wireless network reliability. It defines the received signal quality being lower than a signal power threshold [55]. Following the definition, UCDA reliability simply becomes the ‘*complementary probability event*’ of U-plane and C-plane signal qualities being larger than some signal quality or outage threshold [7]. Thus, in wireless interface, the contributing effects of both the planes are virtually equal. This event happens due to underweighting C-plane contributions for system reliability. C-plane keeping the architecture stable and seamlessly connected deems the conventional outage probability incapable of providing accurate reliability information of UCDA.

5.2.1.2 Unreliability Factor

It has been discussed in previous sections that PDSCH carries the small cell traffic or user plane data whereas, PDCCH transmits the control plane data with macro cells. PDCCH is responsible to correctly encode or decode the data from PDSCH. In PDCCH poorly received signal causes higher Symbol Error Rate (SER). However, high SER eventually will degrade the performance in PDSCH due to failure in correctly

decoding the PDSCH channel data. Therefore, if SER in PDCCH is beyond a certain threshold even having good signal quality in PDSCH will ensure failure in total transmission. Therefore, authors in [55] proposed Unreliability Factor (URF) to provide deserved importance of C-plane and find the reliability of UCDA properly. The dependence is defined through mapping of decoupled architecture based on C-plane as, $SER_{U/C} = \alpha(SER_C)$, where $SER_{U/C}$ is the SER of decoupled architecture mapped into SER of control plane defined as SER_C through α or a mapping function ranging from 0 to 1 with $SER_{U/C}$ having a range from 0 to 1. Based on above discussion, URF can simply defined as,

$$URF = \begin{cases} P(SER_U > th_U), & SER_C \leq th_C \\ 1, & SER_C > th_C \end{cases} \quad (5.1)$$

Where, SER_U is the symbol error rate of the U-plane and th_U and th_C being the signal quality threshold of U-plane and C-plane. From (5.1), it can be verified that beyond a particular threshold of SER_C , the entire architecture is unreliable. Therefore, URF will depend on outage probability of PDSCH given that the outage probability of PDCCH is above some threshold. The outage probability of PDSCH is lower than 1 and at some point $SER_C = th_C$, which makes it, not a probability function [55]. URF is defined more in [55], with detailed mathematical deductions. The reliability relation can be thus explained by Figure 5.4 as, SIR_C and SIR_U being not completely

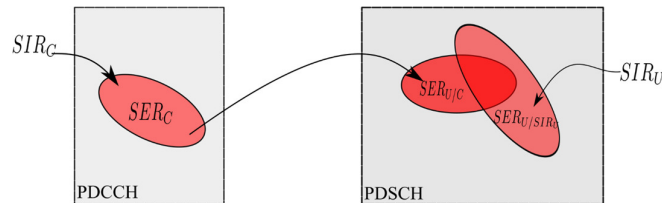


Figure 5.4: Frame mapping and relations

independent and $SER_{U/C}$ and SER_{U/SIR_U} being correlated. Considering conditional independence, it was proposed that,

$$SER_U = SER_{U/C} + SER_{U/SIR_U} - SER_{U/C} \cdot SER_{U/SIR_U} \quad (5.2)$$

In LTE network, for better reliability C-plane Quadrature Phase Shift Keying (QPSK) is used and its SER is denoted by,

$$SER_C = 2Q(\sqrt{2SIR_C})(1 - Q(\sqrt{2SIR_C})) \quad (5.3)$$

Where, $Q(x) = 1 - \Phi(x) = \frac{1}{\sqrt{2\pi}} \int_x^\infty e^{-\frac{t^2}{2}} dt$.

For U-plane, M-QAM ($M \in (4, 16, 64)$) can be used with SER_{U/SIR_U} being denoted by,

$$SER_{U/SIR_U} = 4\left(1 - \frac{1}{\sqrt{M}}\right)Q\left(\sqrt{\frac{3 \log_2 M}{M-1} SIR_U}\right) \quad (5.4)$$

Chapter 6. MULTI-ANTENNA CIRCULAR FIBER-FED FIFO FOR LOGICAL CELL MAPPING (MAC-3FLCM)

As Han *et al.* suggested in RADIATE [34], that in 70 – 140ms RTT the train may move 10m creating high channel variation in high frequency small cell transmissions. The phenomena is shown in RADIATE where the channel variation may occur due to mobility and lead to severe nonstationarity and time varying effects. In a traditional single antenna situation, train moves 10m in each RTT, therefore user will receive the acknowledgement back for each request, when the user moves to a new position 10m away from the first position [34]. This phenomenon will eventually deactivate Channel Quality Indication (CQI) reported to the user side. The scope of RADIATE was to deploy on-roof antenna over train to remove the channel variation from user side. However, this will lead to a redundant deployment of antennas over train. In a 5G small cell scenario, avoiding channel variation through multiple deployment of antennas is not ideal due to high power consumption in beamforming for uplink transmission. In UCDA, user plane on-roof train antennas will use massive multi user MIMO (MU-MIMO) with up to 64 to 256 antenna elements. Due to smaller wavelength mmWave antenna form factor is very small. There is a possibility of strategic deployment of antennas to reduce metallic loss and reduce influence on antenna lobes. In this chapter, background of the MAC-3FLCM architecture, description and mathematical analysis have been given.

6.1. Background

In UCDA, 5G small cells are called '*phantom cells*' due to their sole capability of transmitting and receiving user plane data. In chapter 5, it has been already discussed the reliability of macro cell based control plane is of more importance for seamless connection in the HST communication framework. The specification of 5G mentions a 1ms delay in the future networks. Even if a network can achieve such characteristics in communication, the RTT would be $\leq 1ms$. The train can move to almost $0.1 - 0.28m$ in that RTT, considering the jump from LTE to 5G networks. The traditional LTE, RTT is $15 - 70ms$, in which train can move up to 10m.

5G communication framework may use FBMC waveforms, mmWave, beamforming and MU-MIMO to cope up with future capacity needs in HSR. Considering all the technologies in high-speed train, there needs to be tradeoff in design to constrain the high BER in communication channel. The channel variation also affect the mmWave frequency through very high Doppler shift and spread, leading to ICI in channels. Therefore, conventional dense and sparse multi antennas deployed on-roof may include redundancy and use a significant amount of energy. Secondly, the small cells base stations are nearer to the track than the macro cell BS, which make them easier for dense deployment along the tracks. However, an ultra-dense deployment would lead to a huge number of handovers in a rapid time-varying environment. Therefore, simply employing more number of antennas on BS for massive MIMO, narrow beamforming or putting more number of base stations in cell edges will not solve the problem in high-speed mobility. However, considering the small cells as phantom cells and delegating the control signaling operation to macro cells would change the concept of hard handover in HST environment to soft handovers. In a fast-

moving architecture, such as HST, UCDA faces a number of challenges from the aspect of handovers and excess delay in RTT, which is discussed in the next section.

6.2 Problem Statement

Overall 5G requires a 1ms RTT delay for communication, which is very much advantageous for HST environment. However, even establishing all fiber optics backbone in UCDA, between macro cells, small and macro cells and small cells, the delay in HST environment for the architecture cannot be easily reduced. With more number of small cell base stations under supervision of macro cells, the outage probability also increases with macro cell assisted frequent handovers and changes with constant connection and reconnection between the small cells. Although the small cells are involved in control signaling, due to more number of small cells involved in user plane data transfer, the train small cell antennas have to change uplink and downlink transmission among the small cells. The coverage of cells decrease with the increasing frequency. Using mmWave frequency cells as macro cell assisted small cells, increases the number of small cells massively, increasing outage probability which in turn degrades the communication channel performance in HST environment. The point of using mmWave cells as small cells under macro cells is to increase outage capacity in a train-to-ground network. Decreasing outage probability would increase the capacity to a significant percentage. However, only increasing the number of small cells with densification does not increase the capacity with reliability required in HST environment. Therefore, it is an open challenge to solve the outage probability problem in 5G-UCDA.

Additional to outage probability, the handovers in the architecture also create problems. Though the overhead in signaling decreases in UCDA, handover occurs more

frequently due to macro cell and small cell based handovers and frequent requirement of synchronization due to user and control plane separation of train passenger data. Due to the separation in planes, it requires sophisticated synchronization between planes and data, so that, there is a minimized loss of information. The problems regarding handover and synchronization in UCDA is mentioned in [56] as,

- a) The number of inter-macro cell handover will increase significantly due to hybrid-cellular architecture.
- b) The handover requirement in decoupled architecture is stringent. The user plane handover occurs after the control plane handover. Thus, entire handover occurs within small cell overlapping region. From Figure 6.1, it is clear that the handover occurs at the ‘small cell overlapping’ region. With a dense deployment such as mmWave frequency cells, the time for handover at overlapping area is reduced.

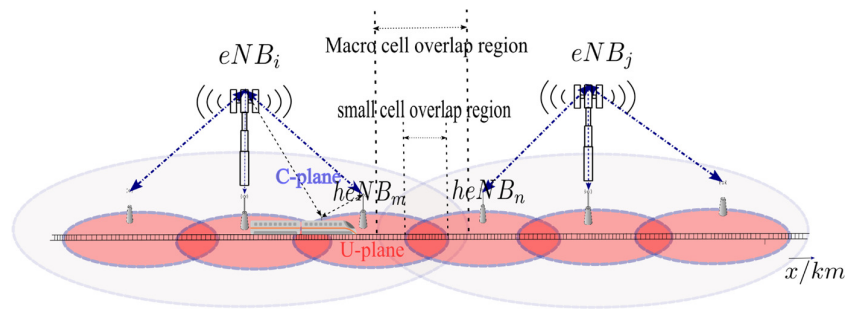


Figure 6.1: Handover scenario in UCDA for overlapping region

- c) In Figure 6.1, two macro cell BS (eNodeB for LTE), are mentioned as eNB_i and eNB_j and small cell BSs as, $heNB_m$ and $heNB_n$. The simultaneous handover trigger, when the power of the signal from eNB_j exceeds that of the signal from the eNB_i . At the same time the power from $heNB_n$ exceeds that from $heNB_m$. Therefore, the handover probability of UCDA at

distance d distance is considered as, $P(d)_{HO} = P_{eNB_i, eNB_j}(d)_{HO} \times P_{heNB_m, heNB_n}(d)_{HO}$. Where, $P_{eNB_i, eNB_j}(d)_{HO}$ is the probability of handover in macro cells, and $P_{heNB_m, heNB_n}(d)_{HO}$ is the handover probability of small cells. The UCDA aggregated handover probability is always lower than the individual handover probability in macro and small cells. Therefore, the handover success probability depends on region of handover. Increasing the size gives an opportunity to increase handover success probability.

In the following section, the MAC-3FLCM architecture is introduced to address the aforementioned challenges.

6.3 The Proposed Architecture

The proposed MAC-3FLCM architecture is based on controlling,

- a) handovers
- b) power consumption
- c) outage probability
- d) decreasing the cell size of mmWave frequency cells to logical cells.

Although the architecture shares certain similarities with RADIATE [34], it reduces the cellular coverage than extending them.

Therefore, we proposed small cell antenna on each rail car for a seamless connection among small cell BS. We also propose to use 5-6 GHz Industrial, Scientific, Medical (ISM) bands or 28 GHz mmWave cells to their maximum cell coverage area 60-200m based on CAPEX and ease of deployment. So that, there are optimized number of small cell BSs that can be deployed to avoid a very dense deployment of

small cells. As we have previously noticed increasing twice the number of BSs will increase the capacity twice. It can be easily be concluded that with increasing densification gain the outage probability would be increasing.

In this architecture, shown in Figure 6.3, which is derived from Figure 6.2, fiber connected on-roof antennas named as AN_i are deployed. The small cells deployed at trackside and on-roof antennas create logical cells relevant to train-to-ground network. All the active on-roof antennas can remain connected to small cells seamlessly. The approach is mentioned as, Multi-antenna Fiber Fed FIFO for Logical Cell Mapping (MAC-3FLCM). The small cells accommodated inside the macro cells can thus be

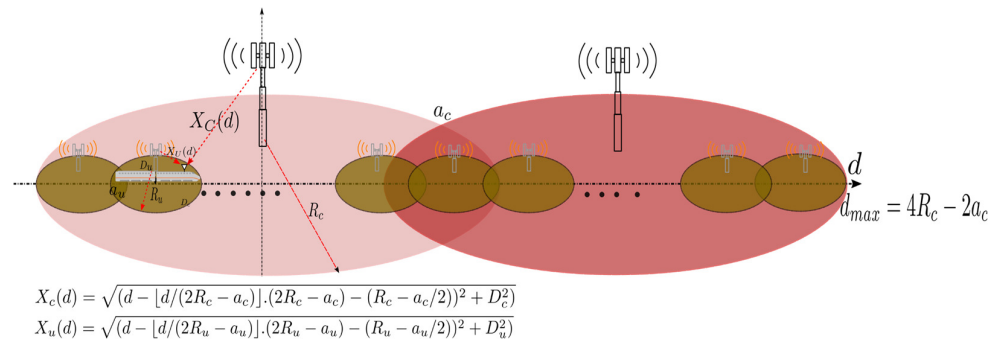


Figure 6.2: Propagation distance variance in UCDA

further reduced based on propagation distance controlled by the on-roof antennas. The access to small cell coverage region is controlled based on linear movement of the train. Therefore, a First in First out approach where, the connection is delegated from the last antenna to the first one can be maintained.

6.3.1 Logical Cells

In different proposals multi-on-roof antennas has been exploited for macro cell BSs or RAUs deployed on macro cell region. But, due to deployment of mmWave cells under supervision of macro cells, the small cells as *phantom cells* can be considered as RAUs with high bandwidth link capabilities, and fiber fed backhaul.

- b) connected on-roof antenna information,
- c) timestamp
- d) Channel state information
- e) transmission success or failure information.

However, the immediate next antenna, in this case AN_2 having femto cell Access Point (AP) connected to it, stores the relayed data by the AN_1 through fiber optic connection. Once AN_1 reaches the linear distance of $\frac{l_{ub}}{2}$, which is the half of the length of the rail cars (or the half distance between two active antennas), the first logical cell is created. Thus the total logical cell coverage becomes l_{ub} , or in this case $22m$. As the control plane keeps a seamless connection in macro cell, only ACK/SYN is required to confirm the transmission and receiving of signals through PDSCH where, PDCCH keeps the seamless connection. With the fiber optic connection among all the antennas, the ACK/SYN commands can be sent among all the active antennas, so that all the in-train APs know which antenna provides the downlink/uplink to train-to-ground small cells. Therefore, in-train APs can relay the user data to appropriate antenna after user and control plane decoupling.

To avoid redundancy, only the on-roof antenna transmits and receives data from the BS in a region of $\frac{l_{ub}}{2}$. After AN_1 leaves the logical cell region of $heNB_1$, AN_2 connects to $heNB_1$ and thus a series of connection have been made by the antennas according to Table 6.1. Until the first antenna AN_1 reaches logical cell coverage of $heNB_2$ and AN_4 leaves the coverage of $heNB_1$, the reconnection does not occur in a new macro cell. However, as we previously discussed, the soft handover in control plane occurs before user plane. Therefore, handover is particularly challenging in overlapping region, which we will be discussing in the next section. For an example only 4 active antennas have been considered to cover a physical cellular region of small cells and

Table 6.1: MAC-3FLCM logical cell mapping

Distance covered by front antenna (d)	BS	DAS
0	$heNB_1$	AN_4
$R_u - l_{ub}/2$	$heNB_1$	AN_4
$R_u + l_{ub}/2$	$heNB_1$	AN_3
$R_u + 3l_{ub}/2$	$heNB_1$	AN_2
$R_u + 5l_{ub}/2$	$heNB_1$	AN_1
$3R_u - a_u - x$	$heNB_1$	AN_4

provide a seamless connection. For Table 6.1, it is assumed that $x \leq \frac{l_{ub}}{2}$.

6.3.2 Proposed Handover Scheme

The handover in this architecture is challenging as, AN_1 is connected to $heNB_2$ and AN_4 is connected to $heNB_1$, control plane would have already switched over to next macro cell base station at macro cell overlapping region a_c . Using a multi-antenna scheme in UCDA, we propose two different solution for user plane handover,

i) CoMP in macro cell overlapping region, ii) Forwarding and synchronization in macro cell region.

Therefore, we provide two ways to discuss this solution, which are mentioned below as,

- a) *CoMP Handover*: From LTE rel. 11 CoMP handover can be done with geographically separated region as previously mentioned and referenced [17, 30, 31]. Dual macro cell on-roof antennas can be used at the same position as first and last active small cell on-roof antennas. The dual antennas can be used to use the CoMP handover scheme method to change the handover information between each other and keep an exact synchronization. In this method, AN_4 do not handover the user plane to AN_1 in a circular FIFO manner until macro cell initiates a complete handover request for CoMP architecture. In this handover solution which is shown in Figure 6.4, the handover is depicted based on bi-casting or CoMP and multiple on-roof antennas. The S-GW is responsible for data packet routing and forwarding between small cells without any control information. Therefore, 1) MME requires to keep connection context information about multiple on-roof antenna units, as, there can be multiple active train antennas capable of connecting to serving and target small cell BSs in a small period of time. 2) S-GW keeps multiple routing table accommodating multiple forwarding path, with copies retained at target and serving BS. Following stages are explained for multi-antenna CoMP handover scheme,
- i) *Handover preparation*: MME being part of the macro cells, the handover for user plane is initiated by the macro cells, with

measurement report directly sent to macro cells periodically. Macro cell decides when to hand over in this scheme. Before triggering the handover it sends a CoMP request message to the target small cell.

- ii) *Handover Execution:* The macro cell requests bi-casting downlink packets from S-GW, where, duplicated packets are sent to AN_4 by

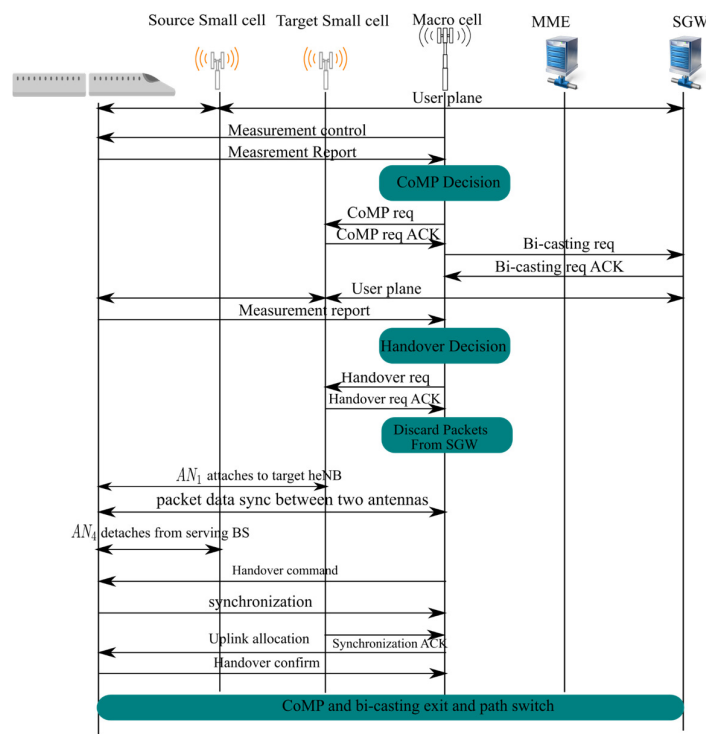


Figure 6.4: CoMP handover for proposed MAC-3FLCM

serving small cell BS for time being. The original is discarded by the target small cell BS, until it becomes serving BS. The handover request is sent from the macro cell to target small cell BS triggering the handover. AN_1 performs synchronization to the target BS. Whenever, AN_4 crosses the logical cell region of $heNB_m$, AN_1 is selected as main user plane communication link.

- iii) *Seamless connection:* It can be possible to transmit and receive data through $AN_2 - AN_4$, while AN_1 enters into logical cell region of

$heNB_n$, and prepares for handover through macro and target small cell BS.

- b) *Forwarding and Synchronization*: As per handover is required in overlapping region, an accurate synchronization can be visualized with the deployment of small cells in macro cells that the control plane handover triggers the user plane handover immediately. Therefore, macro cell antenna needs a strategic placement. In our MAC-3FLCM architecture there is no physical small cell overlapping area. Therefore, after a disconnection from AN_1 , AN_2 will proceed with further user plane data uplink/downlink with control plane data transfer towards eNB_2 . It can be possible with the help of SGW, a time synchronized or sequential change of small cell target BS and connecting on-roof antenna. As the distance between the antennas are assumed as, l_{ub} , in each $\frac{l_{ub}}{v}$ s, it can be possible for consecutive reconnection with on-roof antennas in FIFO manner without intervention from macro cells. However, in overlapping region CoMP handover will reduce additional forwarding delay in in-train network. Therefore, change of handover scheme is required.

The only point of failure is when there is hard handover in macro cells. The time required for handing over control signal of user plane information of passenger data may create serious synchronization issue as the small cell antenna will seamless transmit/receive information. Therefore, during handover a buffer request may solve the synchronization problem.

6.3.3 Power Control

Due to usage of logical cells instead of physical cells the power consumption of mmWave cells can be reduced heavily. Due to highly directional and analog beamforming methods, the entire process can be time consuming. Large array massive MIMO antennas to avoid Doppler shift and spread in the channel will also be used in train-to-ground communication receiver and transmitter sides. Therefore, a large power consumption trend can be seen. However, using MAC-3FLCM schemes to vary frequency along a multi-frequency 5G deployment scenario where different high frequency small cells can be used and a constrained power control scheme can be drawn. In higher frequencies the air attenuation loss, fog and rain loss being significant communication reliability depends on the distance. Logical cell architecture reduces the number of cells and reduces the coverage so that a lower transmitting power can be used. With lower transmitting power, and large number of arrays, the power in the architecture can be effectively controlled and receiver complexity can also be significantly reduced.

6.4 Analysis of the Proposed Architecture

Assuming a train start its journey from $d = 0$ to $d = 4R_c - 2a_c$, where R_c is the control plane coverage and a_c is the overlapping region as mentioned in Figure 6.2. The proposed UCDA model, where control plane propagation distance $X_c(d)$ and user plane propagation distance $X_u(d)$ varies as,

$$X_c(d) \tag{6.1}$$

$$= \sqrt{\left(d - \left\lfloor \frac{d}{2R_c - a_c} \right\rfloor \cdot (2R_c - a_c) - \left(R_c - \frac{a_c}{2}\right)\right)^2 + D_c^2}$$

$$X_u(d) \tag{6.2}$$

$$= \sqrt{\left(d - \left\lfloor \frac{d}{2R_u - a_u} \right\rfloor \cdot (2R_u - a_u) - \left(R_u - \frac{a_u}{2}\right)\right)^2 + D_u^2}$$

Where, D_c and D_u denote track to macro and small cell distances. Therefore, theoretically we can assume $heNB_1$ is the first small cell Bsin its path. Individual path loss can be assumed for Hata and CIR from (3.2) for 5G cells as,

$$PL_c(d) = PL_{c0}(d_0) + 10n\log_{10}(X_c(d)) + \sigma_c \tag{6.3}$$

$$PL_u(d) = PL_{CIR}(X_u(d)) \tag{6.4}$$

Where n is dependent on macro cell environment, which is mostly considered as suburban ($n = 2$), σ_c is the log-normal shadowing, d_0 is the reference distance and $PL_{c0}(d_0)$ is the Hata path loss at reference distance. The respective receiver powers are given by (6.5) and (6.6),

$$P_{recv_c} = Pt_c - PL_c(d) \tag{6.5}$$

$$P_{recv_u} = Pt_u - PL_u(d) \tag{6.6}$$

Where, Pt_c and Pt_u are transmitter control and user plane cells. Therefore, their respective Signal-to-Interference (SIR) would be (channel to be considered interference-limited),

$$SIR_c = 10^{(Pt_c - PL_c(X_c(d)) - 10\log_{10}(I_c))} \tag{6.7}$$

$$SIR_u = 10^{(Pt_u - PL_u(X_u(d)) - 10 \log_{10}(I_u))} \quad (6.8)$$

Where, $I = \sum_{i=1}^{nIS} I_i$, is the co-channel interference for each plane considering a linear arrangement of base stations and nIS being the number of BSs. In our proposed MAC-3FLCM architecture, the logical cell mapping can be done with user plane propagation distance varying as in (6.9),

$$(6.9)$$

Therefore, the path loss becomes significantly less due to smaller propagation distance. The SIR_u value changes towards a better value, contributing to better outage probability and thus outage capacity. Outage probability is defined as,

$$\begin{aligned} P_{out}(d) &= P[Pt - PL(d) - I + X_\sigma < \Gamma] \\ &= \Phi\left[\frac{\Gamma + I + PL(d) - Pt}{\sigma}\right] \end{aligned} \quad (6.10)$$

Equation (6.10) shows a trivial scenario for both the planes, where, $\Phi(x) = \int_{-\infty}^x \frac{\exp\left(-\frac{t^2}{2}\right)}{\sqrt{2\pi}}$ and X_σ is a normal Gaussian normal distribution with zero mean and variance σ . Assuming individual outage probability for macro and small cells as P_m and P_s , the control and user plane decoupling would result in a total outage probability of decoupled architecture of $P_{U/C} = 1 - (1 - P_m) \cdot (1 - P_s)$, where macro cells carry the control plane information for both train and passengers and small cells carry only the user plane information of passengers. Now for the sake of comparison, if small cells carry both user and control plane information, it would lead to an outage probability of $P_{out_{sc}} = 1 - (1 - P_s) \cdot (1 - P_s)$. Due to higher pathloss in higher frequencies, 5G

base stations contribute to a higher outage probability thus a higher outage capacity. The user plane may seem unstable due to its higher unreliability in the network. Finally, the outage capacity can be calculated for proposed MAC-3FLCM is in trivial form, $C(x) = (1 - p_{U/C}) \cdot BW \cdot \log_2(1 + SIR_{U/C}(d))$, where, the cumulative capacity is the sum of the individual outage capacity, BW is the accumulated bandwidth, $p_{U/C}$ is the outage probability of decoupled architecture and $SIR_{U/C}$ is the signal to interference ratio in UCDA.

6.5 Simulation Results

The analysis has been done assuming only general communication schemes,

Table 6.2: Simulation parameters

Parameters	Macro	Small
Coverage (R_c, R_u)	1 km	0.11 km
Overlap (a_c, a_u)	0.2 km	0.016 km
Frequency (f_c, f_u)	2 GHz	28 GHz
Bandwidth (BW_c, BW_u)	20 MHz	1 GHz
Distance from track (D_c, D_u)	0.030	0.02
Path loss model	Hata	CI
Connection outage threshold (Γ_c, Γ_u)	6 dB	8dB
Shadow fading variance (σ_c, σ_u)	4 dB	8 dB
Transmitter power (Pt_c, Pt_u)	43 dBm	43 dBm
$PLE(CI)$	3.1	
Train length (t_l)	400 m	
No. of cars (n_{car})	18	

and do not consider paging or handover. Table 6.2 shows the simulation parameters.

The simulation results in Figure 6.5 shows that there is a drastic increase in capacity.

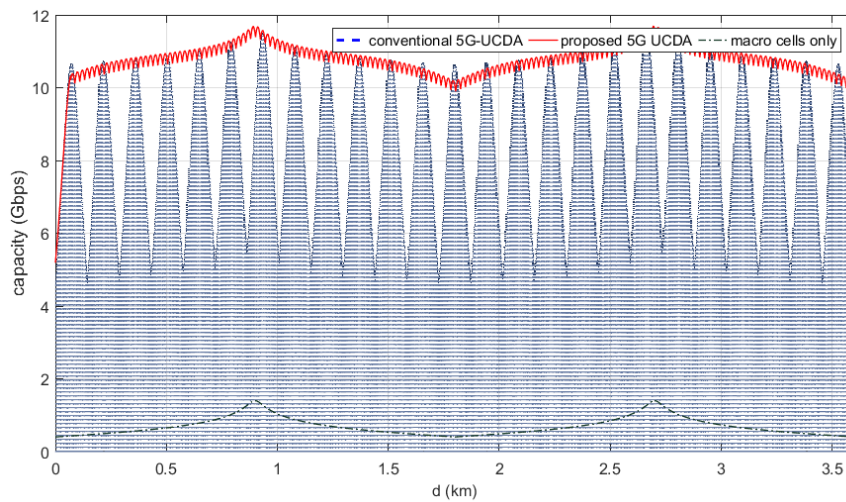


Figure 6.5: Comparison of capacity in the architectures

In a conventional macro cell only network the capacity can achieved near to 12 Gbps,

whereas using 28 GHz small cells in macro cell assisted decoupled architecture, the capacity can achieve around 10 Gbps. However the capacity is only near to 10 Gbps when it is close to small cell BS. Due to high path loss in small cells and high outage probability further from BS, the capacity drops far from BS. Considering reliability of macro cells along with small cells, the capacity may drop to unusable percentage. Even though the capacity increase to 5-10 fold than macro cell only network, there is a significant fluctuation. Figure 6.6 shows the outage probability, in which as it is discussed, macro cells show a reliable nature. Using only mmWave small cells increase the outage probability to a significant measure. Even using UCDA, the outage

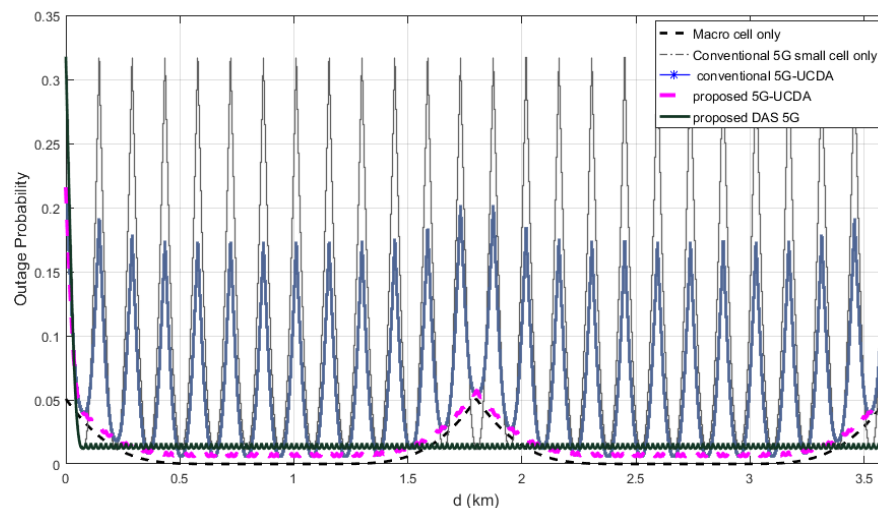


Figure 6.6: Comparison of outage probability in the architectures probability keeps the system unreliable. If we consider the Figure 6.6 and 6.7 in detail, we can observe that the outage capacity drops significantly at edges with outage probability being maximum at the edges. This happens due to high pathloss of higher frequency cells. The pathloss increases with the propagation distances increasing

further from BS. The area spectral efficiency being dependent on the area involved, also decreases significantly. The effect of cell coverage can be observed in Figure 6.7.

With increasing coverage area, all small cell related outage probability decreases. This

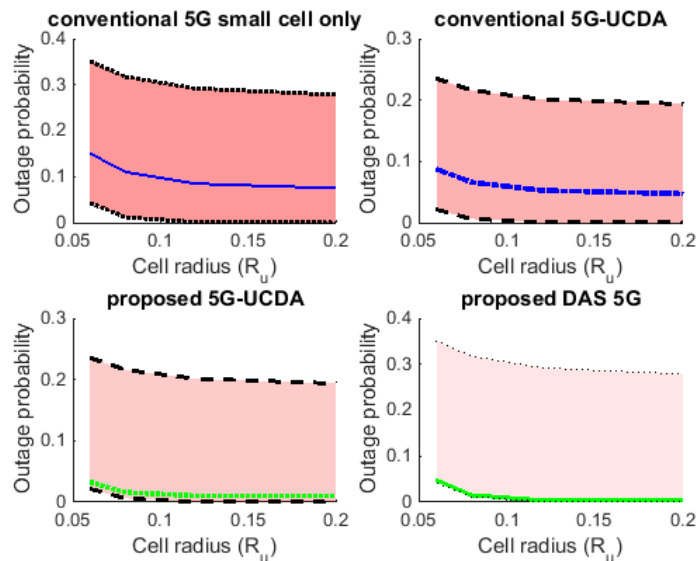


Figure 6.7: Comparison of outage probability in different architectures based on cell radius

may seem counterintuitive. However, with higher coverage area we need to deploy less number of small cell BSs in place resulting in less interference integrating to the communication channel. A dense deployment means more inter-cell interference. Therefore, we eventually observe a high outage probability in smaller coverage area cells and with less number of small cells outage probability improves.

Therefore, our proposed architecture work with any arbitrary densification factors and mmWave frequencies. The proposed architecture simultaneously decreases the physical cell to logical cell and extends the logical cell coverage by the multi-antennas, so that, the signal from small cell BS do not face severe path loss. There is a seamless connection between on-roof antennas and small cell BS with 95% improvement in outage probability and constant 10Gbps outage capacity. It can be

concluded that without a number of complex massive MIMO deployed on-roof, MAC-3FLCM can provide an optimum future-proof performance. Comparing with RADIATE, which deploys multiple antenna at every 10m for Doppler shift reduction, MAC-3FLCM focused on power control, outage probability, outage capacity and area spectral efficiency. Our results show that with increasing small cell coverage, outage probability decreases due to less number of small cell BSs in a macro cell. However, controlling, creating and extending logical cell coverage with multi-antenna scheme contribute toward spectral efficiency as, outage capacity being much higher than conventional schemes for a lower logical cell region. It can be noted MAC-3FLCM 5G small cell only architecture has lower outage probability trend than 5G MAC-3FLCM UCDA. The contributing outage of C-plane increases the outage probability of MAC-3FLCM UCDA than macro cell only outage probability.

6.6 Discussions

The proposed architecture with 5G-UCDA increases overall reliability of the HST communication, assuming there is also passenger or bandwidth intensive communication involved. Conventional UCDA does not provide guaranteed reliability for a dense deployment where HST communication schemes will attempt to attain the high spectral efficiency available with mmWave small cells. Our goal was with MAC-3FLCM to achieve outage probability close to macro cells. On-roof antennas on rail cars can communicate with small cell BS within logical cells made by them and extend their region with on-roof antennas. But with minimal number of active on-roof antennas the feasibility of deployment as in-train and train to ground antennas design also remains attainable. With our proposed architecture, we could achieve the following advantages,

- a) It provides a seamless connection depending on macro cell BSs
- b) It achieves 95% improvement from conventional UCDA outage probability
- c) MAC-3FLCM design architecture fits perfectly with mechanical design of trains. Considering small cell RTT of 1ms, HST moves .1-.28m and considering an average 10ms RTT the train will move 10-28m, which is average length of a rail car and distance of two active antennas in MAC-3FLCM. Therefore, Doppler shift can be avoided based on RADIATE architecture [34]
- d) A constant capacity of 10Gbps is maintained in MAC-3FLCM without any sheer drops. However, the architecture will be future proof and capable of supporting tactile internet in most mobile internet considering clustered active antennas
- e) It also improved the spectral efficiency to 10-15-fold due to decreasing size of logical cells
- f) The architecture also support avid power control due to logical cell size being less than the physical coverage and adaptable transmit power can be used to vary physical cell coverage
- g) The antennas can be designed to make them small cell frequency independent to optimize CAPEX with different country using different frequency small cell arrangements.
- h) There are soft handover schemes involved adding very low latency in MAC-3FLCM and supports the 5G architecture for sub-millisecond delay.
- i) The search size for angular location can be reduced for beamforming.

6.7 Future Work

The future work involves a simulation considering wideband non-stationary MIMO environment with primary and secondary scatterers involved in the network. Further simulation involves, time invariant channel characteristics, small scale fading considerations, different channel environments and Doppler shift estimation. We will also consider FBMC for further developing a link-to-link communication scheme where user plane SER will be considered for OQAM. The drastic drop in SER due to use of OQAM will guarantee a better reliability in user plane.

6.8 Conclusions

In this thesis, we discussed the challenges of high-speed train wireless channel environment and the latest methods proposed in literature to address these challenges. The main goal of this thesis is to provide uninterrupted passengers in high-speed trains, wireless broadband services with very low latency and guaranteed quality of service. This is to attain a modular, flexible, interoperable train centric network architecture that can assure train control/signaling/braking service to operate seamlessly. In the thesis, we have studied the potential of implementation of fifth generation wireless communication systems in high-speed environment. The disruptive nature of the 5G communication to guarantee very low latency and high bandwidth to support increasing device centric traffic load have been stressed to figure out if it can withstand high speed mobility related challenges. New generation waveforms and modulation have been studied and identified to map them to train related services. Our research also identifies the waveforms, antenna deployments/diversity, handover methods and novel logical

cell based linear coverage architecture to cope up with high-speed mobility without any degradation in reliability.

We have proposed an architecture that is novel based on visualizing non-overlapping linear coverage of cells. We also proposed on-roof multi-antenna deployment without diversity to adaptably control logical cellular region of the cells with a novel handover scheme. In a conventional dual link user and control plane separated architecture, small cells are responsible for carrying high bandwidth passenger user plane data or data without any control information, whereas, macro cells carry the control data of train control and passenger control plane data. In conventional architectures, the reliability and densification gains are biased, due to their better efficiency nearby base stations. In our Multi Antenna Circular Fiber Fed FIFO Logical Cell Mapping (MAC-3FLCM) scheme, we removed this biasness and retained the best possible performance from the network in terms of capacity, reliability, and spectral efficiency. The proposed architecture can attain a 10-15-fold improvement in spectral efficiency and 95% improvement in reliability than conventional architectures. Better spectral efficiency and possibility of controlling it, ensures also power control in the architecture by reducing the physical cell size to its logical cell size.

REFERENCES

- [1] Banerjee, S., & Sharif, H. (2016). A Survey of Wireless Communication Technologies & Their Performance for High-speed Railways. *Journal of Transportation Technologies*, 6(01), 15.
- [2] High-speed - UIC - International union of railways. (2017). UIC - International union of railways. Retrieved 1 April 2017, from <http://www.uic.org/highspeed>

- [3] Ai, B., Cheng, X., Kürner, T., Zhong, Z. D., Guan, K., He, R. S., ... & Briso-Rodriguez, C. (2014). Challenges toward wireless communications for high-speed railway. *IEEE Transactions on Intelligent Transportation Systems*, 15(5), 2143-2158.
- [4] "WINNER II channel models," IST-WINNER II, Munich, Germany, Tech. Rep. Deliverable 1.1.2 v.1.2, Feb. 2008.
- [5] He, R., Ai, B., Zhong, Z., Molisch, A. F., Chen, R., & Yang, Y. (2015). A measurement-based stochastic model for high-speed railway channels. *IEEE Transactions on Intelligent Transportation Systems*, 16(3), 1120-1135.
- [6] Conformance specification Radio, U. E. U. (2012). 3rd Generation Partnership Project; Technical Specification Group Radio Access Network; Evolved Universal Terrestrial Radio Access (E-UTRA); User Equipment (UE) conformance specification Radio transmission and reception.
- [7] Goldsmith, A. (2005). *Wireless communications*. Cambridge university press.
- [8] Ghazal, A., Yuan, Y., Wang, C. X., Zhang, Y., Yao, Q., Zhou, H., & Duan, W. (2016). A Non-Stationary IMT-A MIMO Channel Model for High-Mobility Wireless Communication Systems. *IEEE Transactions on Wireless Communications*.
- [9] Ghazal, A. (2015). *Propagation channel characterisation and modelling for high-speed train communication systems* (Doctoral dissertation, Heriot-Watt University).
- [10] Ghazal, A., Wang, C. X., Ai, B., Yuan, D., & Haas, H. (2015). A nonstationary wideband MIMO channel model for high-mobility intelligent transportation systems. *IEEE Transactions on Intelligent Transportation Systems*, 16(2), 885-897.
- [11] Sayeed, A. M., & Raghavan, V. (2007). Maximizing MIMO capacity in sparse multipath with reconfigurable antenna arrays. *IEEE Journal of Selected Topics in Signal Processing*, 1(1), 156-166.
- [12] Rodriguez-Pineiro, J., Domnguez-Bolano, T., Suarez-Casal, P., Garcia-Naya, J. A., & Castedo, L. (2016, March). Affordable evaluation of 5G modulation schemes in

high-speed train scenarios. In Smart Antennas (WSA 2016); Proceedings of the 20th International ITG Workshop on (pp. 1-8). VDE.

- [13] Rodriguez-Pineiro, J., Suárez-Casal, P., Lerch, M., Caban, S., Garcia-Naya, J. A., Castedo, L., & Rupp, M. (2015, May). LTE downlink performance in high-speed trains. In Vehicular Technology Conference (VTC Spring), 2015 IEEE 81st (pp. 1-5). IEEE.
- [14] Calle-Sánchez, J., Molina-García, M., Alonso, J. I., & Fernández-Durán, A. (2013). Long term evolution in high-speed railway environments: Feasibility and challenges. *Bell Labs Technical Journal*, 18(2), 237-253.
- [15] He, R., Ai, B., Wang, G., Guan, K., Zhong, Z., Molisch, A. F., ... & Oestges, C. P. (2016). High-Speed Railway Communications: From GSM-R to LTE-R. *Ieee vehIcular technology magazIne*, 11(3), 49-58.
- [16] Fan, P., Zhao, J., & Chih-Lin, I. (2016). 5G high mobility wireless communications: Challenges and solutions. *China Communications*, 13(Supplement2), 1-13.
- [17] Luo, W., Zhang, R., & Fang, X. (2012). A CoMP soft handover scheme for LTE systems in high-speed railway. *EURASIP Journal on Wireless Communications and Networking*, 2012(1), 1-9.
- [18] Zhang, Y., He, Z., Zhang, W., Xiao, L., & Zhou, S. (2014). Measurement-based delay and Doppler characterizations for high-speed railway hilly scenario. *International Journal of Antennas and Propagation*, 2014.
- [19] Banerjee, S., Hempel, M., & Sharif, H. (2017). Decoupled U/C Plane Architecture for HetNets and High-speed Mobility: Research Directions & Challenges, *Consumer Communications & Networking Conference (CCNC)*, IEEE (accepted, to be published)

- [20] KG, R. (2017). 5G Waveform Candidates - Application Note - 1MA271. Rohde-schwarz.com. Retrieved 2 April 2017, from <http://www.rohde-schwarz.com/appnote/1MA271>
- [21] Lannoo, B., Colle, D., Pickavet, M., & Demeester, P. (2007). Radio-over-fiber-based solution to provide broadband internet access to train passengers [Topics in Optical Communications]. *IEEE Communications Magazine*, 45(2), 56-62.
- [22] Li, G., Guan, K., Ai, B., He, D., He, R., Hui, B., ... & Zhong, Z. (2016, October). On the high-speed railway communication at 30 GHz band: Feasibility and channel characteristics. In *Antennas, Propagation and EM Theory (ISAPE), 2016 11th International Symposium on* (pp. 796-799). IEEE.
- [23] Pleros, N., Tsagkaris, K., & Tselikas, N. D. (2008). A moving extended cell concept for seamless communication in 60 GHz radio-over-fiber networks. *IEEE Communications Letters*, 12(11).
- [24] Wang, J., Zhu, H., & Gomes, N. J. (2012). Distributed antenna systems for mobile communications in high-speed trains. *IEEE Journal on Selected Areas in Communications*, 30(4), 675-683.
- [25] Chow, B., Yee, M. L., Sauer, M., Ng'Oma, A., Tseng, M. C., & Yeh, C. H. (2009, July). Radio-over-fiber distributed antenna system for WiMAX bullet train field trial. In *Mobile WiMAX Symposium, 2009. MWS'09*. IEEE (pp. 98-101). IEEE.
- [26] Khan, A., & Jamalipour, A. (2016). An Outage Performance Analysis with Moving Relays on Suburban Trains for Uplink. *IEEE Transactions on Vehicular Technology*.
- [27] Lee, C. W., Chuang, M. C., Chen, M. C., & Sun, Y. S. (2014). Seamless handover for high-speed trains using femtocell-based multiple egress network interfaces. *IEEE Transactions on Wireless Communications*, 13(12), 6619-6628.

- [28] Lee, C. W., Chuang, M. C., Chen, M. C., & Sun, Y. S. (2014). Seamless handover for high-speed trains using femtocell-based multiple egress network interfaces. *IEEE Transactions on Wireless Communications*, 13(12), 6619-6628.
- [29] Ishii, H., Kishiyama, Y., & Takahashi, H. (2012, December). A novel architecture for LTE-B: C-plane/U-plane split and phantom cell concept. In *Globecom Workshops (GC Wkshps)*, 2012 IEEE (pp. 624-630). IEEE.
- [30] Yan, L., Fang, X., & Fang, Y. (2015). Control and data signaling decoupled architecture for railway wireless networks. *IEEE Wireless Communications*, 22(1), 103-111.
- [31] Yang, C., Lu, L., Di, C., & Fang, X. (2010, September). An on-vehicle dual-antenna handover scheme for high-speed railway distributed antenna system. In *Wireless Communications Networking and Mobile Computing (WiCOM)*, 2010 6th International Conference on (pp. 1-5). IEEE.
- [32] Tian, L., Li, J., Huang, Y., Shi, J., & Zhou, J. (2012). Seamless dual-link handover scheme in broadband wireless communication systems for high-speed rail. *IEEE Journal on Selected Areas in Communications*, 30(4), 708-718.
- [33] Luo, W., Fang, X., Cheng, M., & Zhao, Y. (2013). Efficient multiple-group multiple-antenna (MGMA) scheme for high-speed railway viaducts. *IEEE Transactions on Vehicular Technology*, 62(6), 2558-2569.
- [34] Han, T., & Ansari, N. (2015). RADIATE: Radio over fiber as an antenna extender for high-speed train communications. *IEEE Wireless Communications*, 22(1), 130-137.
- [35] Vision, I. M. T. (2014). Framework and overall objectives of the future development of IMT for 2020 and beyond. ITU, Feb.
- [36] Andrews, J. G., Buzzi, S., Choi, W., Hanly, S. V., Lozano, A., Soong, A. C., & Zhang, J. C. (2014). What will 5G be?. *IEEE Journal on selected areas in communications*, 32(6), 1065-1082.

- [37] Sun, S., MacCartney, G. R., & Rappaport, T. S. (2016, April). Millimeter-wave distance-dependent large-scale propagation measurements and path loss models for outdoor and indoor 5G systems. In *Antennas and Propagation (EuCAP), 2016 10th European Conference on* (pp. 1-5). IEEE.
- [38] Sun, S., Rappaport, T. S., Rangan, S., Thomas, T. A., Ghosh, A., Kovacs, I. Z., ... & Jarvelainen, J. (2016, May). Propagation path loss models for 5G urban micro-and macro-cellular scenarios. In *Vehicular Technology Conference (VTC Spring), 2016 IEEE 83rd* (pp. 1-6). IEEE.
- [39] Sulyman, A. I., Nassar, A. T., Samimi, M. K., Maccartney, G. R., Rappaport, T. S., & Alsanie, A. (2014). Radio propagation path loss models for 5G cellular networks in the 28 GHz and 38 GHz millimeter-wave bands. *IEEE Communications Magazine*, 52(9), 78-86.
- [40] Kela, P., Gelabert, X., Turkka, J., Costa, M., Heiska, K., Leppänen, K., & Qvarfordt, C. (2016, May). Supporting mobility in 5G: A comparison between massive MIMO and continuous ultra dense networks. In *Communications (ICC), 2016 IEEE International Conference on* (pp. 1-6). IEEE.
- [41] Liu, Y., Zhang, Y., Ghazal, A., Wang, C. X., & Yang, Y. (2016, May). Statistical Properties of High-Speed Train Wireless Channels in Different Scenarios. In *Vehicular Technology Conference (VTC Spring), 2016 IEEE 83rd* (pp. 1-5). IEEE.
- [42] Marzetta, T. L. (2010). Noncooperative cellular wireless with unlimited numbers of base station antennas. *IEEE Transactions on Wireless Communications*, 9(11), 3590-3600.
- [43] Kutty, S., & Sen, D. (2016). Beamforming for millimeter wave communications: An inclusive survey. *IEEE Communications Surveys & Tutorials*, 18(2), 949-973.
- [44] Gabor, D. (1946). Theory of communication. Part 1: The analysis of information. *Journal of the Institution of Electrical Engineers-Part III: Radio and Communication Engineering*, 93(26), 429-441.

- [45] Viholainen, A.; Bellanger, M.; Huchard, M.; "PHYDAS - PHYsical layer for Dynamic AccesS and cognitive radio", Report D5.1, January 2009
- [46] Schaich, F. (2010, April). Filterbank based multi carrier transmission (FBMC)—evolving OFDM: FBMC in the context of WiMAX. In *Wireless Conference (EW), 2010 European* (pp. 1051-1058). IEEE.
- [47] Schaich, F., & Wild, T. (2014, May). Waveform contenders for 5G—OFDM vs. FBMC vs. UFMC. In *Communications, Control and Signal Processing (ISCCSP), 2014 6th International Symposium on* (pp. 457-460). IEEE.
- [48] Vakilian, V., Wild, T., Schaich, F., ten Brink, S., & Frigon, J. F. (2013, December). Universal-filtered multi-carrier technique for wireless systems beyond LTE. In *Globecom Workshops (GC Wkshps), 2013 IEEE* (pp. 223-228). IEEE.
- [49] Gaspar, I. S., Mendes, L. L., Michailow, N., & Fettweis, G. (2014). A synchronization technique for generalized frequency division multiplexing. *EURASIP Journal on Advances in Signal Processing*, 2014(1), 67.
- [50] 5G-Now. Deliverable D3.2 : 5G waveform candidate selection. Technical report, 5G Now (5th Generation Non-Orthogonal Waveforms for Asynchronous Signalling), 2015.
- [51] Wunder, G., Jung, P., Kasparick, M., Wild, T., Schaich, F., Chen, Y., ... & Mendes, L. (2014). 5GNOW: non-orthogonal, asynchronous waveforms for future mobile applications. *IEEE Communications Magazine*, 52(2), 97-105.
- [52] 5G Channel Model Simulator Software | NYU WIRELESS. (2017). NYU WIRELESS. Retrieved 2 April 2017, from <http://wireless.engineering.nyu.edu/5g-millimeter-wave-channel-modeling-software>
- [53] Kishiyama, Y., Benjebbour, A., Nakamura, T., & Ishii, H. (2013). Future steps of LTE-A: Evolution toward integration of local area and wide area systems. *IEEE Wireless Communications*, 20(1), 12-18.

- [54] Yan, L., & Fang, X. (2013, November). Decoupled wireless network architecture for high-speed railway. In High Mobility Wireless Communications (HMWC), 2013 International Workshop on (pp. 96-100). IEEE.
- [55] Yan, L., & Fang, X. (2014). Reliability evaluation of 5G C/U-plane decoupled architecture for high-speed railway. *EURASIP Journal on Wireless Communications and Networking*, 2014(1), 1-11.
- [56] Song, H., Fang, X., & Yan, L. (2014). Handover scheme for 5G C/U plane split heterogeneous network in high-speed railway. *IEEE Transactions on Vehicular Technology*, 63(9), 4633-4646.
- [57] Zhang, J. Y., Tan, Z. H., Zhong, Z. D., & Kong, Y. (2010, September). A multi-mode multi-band and multi-system-based access architecture for high-speed railways. In *Vehicular Technology Conference Fall (VTC 2010-Fall)*, 2010 IEEE 72nd (pp. 1-5). IEEE.